The Plant Cell, Vol. 19: 731–749, March 2007, www.plantcell.org © 2007 American Society of Plant Biologists

RESEARCH ARTICLES

Analysis of Transcription Factor HY5 Genomic Binding Sites Revealed Its Hierarchical Role in Light Regulation of Development [W]

Jungeun Lee,[a,b,1] Kun He,[c,1] Viktor Stolc,[a,d] Horim Lee,[b] Pablo Figueroa,[a] Ying Gao,[a,c] Waraporn Tongprasit,[e] Hongyu Zhao,[f] Ilha Lee,[b,2] and Xing Wang Deng[a,c,2]

[a] Department of Molecular, Cellular, and Developmental Biology, Yale University, New Haven, Connecticut 06520-8104
[b] Department of Biological Sciences, Seoul National University, Seoul 151-742, Korea
[c] Peking–Yale Joint Center of Plant Molecular Genetics and Agrobiotechnology, Center for Bioinformatics, National Laboratory of Protein Engineering and Plant Genetic Engineering and College of Life Sciences, Peking University, Beijing 100871, People's Republic of China
[d] Genome Research Facility, NASA Ames Research Center, Moffett Field, California 94035
[e] Eloret Corporation, Sunnyvale, California 94087
[f] Department of Epidemiology and Public Health, School of Medicine, Yale University, New Haven, Connecticut 06520

The transcription factor LONG HYPOCOTYL5 (HY5) acts downstream of multiple families of the photoreceptors and promotes photomorphogenesis. Although it is well accepted that HY5 acts to regulate target gene expression, in vivo binding of HY5 to any of its target gene promoters has yet to be demonstrated. Here, we used a chromatin immunoprecipitation procedure to verify suspected in vivo HY5 binding sites. We demonstrated that in vivo association of HY5 with promoter targets is not altered under distinct light qualities or during light-to-dark transition. Coupled with DNA chip hybridization using a high-density 60-nucleotide oligomer microarray that contains one probe for every 500 nucleotides over the entire *Arabidopsis thaliana* genome, we mapped genome-wide in vivo HY5 binding sites. This analysis showed that HY5 binds preferentially to promoter regions in vivo and revealed >3000 chromosomal sites as putative HY5 binding targets. HY5 binding targets tend to be enriched in the early light-responsive genes and transcription factor genes. Our data thus support a model in which HY5 is a high hierarchical regulator of the transcriptional cascades for photomorphogenesis.

INTRODUCTION

As sessile organisms, higher plants have evolved highly plastic developmental programs in response to a changing environment. The most influential environmental factor is probably light, which is used as an informational signal as well as an energy source for plants (reviewed in Kendrick and Kronenberg, 1994). Light affects plant growth and development throughout the entire life cycle from germination to flowering (Smith, 2000; Sullivan et al., 2003). To monitor the surrounding light conditions, plants have at least four classes of photoreceptors: red (R)/far-red (FR) light–sensing phytochrome (phy) family, blue/UV-A light–sensing cryptochromes, phototropins, and UV-B light–sensing yet uncharacterized photoreceptor (Sullivan et al., 2003; Chen et al., 2004).

A microarray analysis using *Arabidopsis thaliana* showed that a massive change in gene expression occurs during photomorphogenesis: up to one-third of the genes in *Arabidopsis* showed changes in expression between light- and dark-grown seedlings (Ma et al., 2001). Similarly, phytochromes regulate the expression of >10% of the genes in *Arabidopsis* in response to continuous red (Rc) or continuous far red (FRc) light (Tepperman et al., 2001, 2004). Interestingly, the analysis of temporal changes in the genomic expression profile in response to R or FR light showed that a large fraction of the genes responding to the light signal within 1 h are transcription factors, including *LONG HYPOCOTYL5* (*HY5*), *CIRCADIAN CLOCK–ASSOCIATED PROTEIN1* (*CCA1*), and *LATE ELONGATED HYPOCOTYL* (*LHY*), which are well-known light signaling components (Tepperman et al., 2001, 2004). This finding suggests that a massive change in gene expression during photomorphogenic development involves transcriptional cascades such that the photoreceptor regulates a master set of transcriptional regulators, which in turn control the expression of multiple downstream target genes. Consistently, the extensive genetic and molecular analyses of light signaling have revealed myriad transcription factors involved in the light control of gene expression (Quail, 2002; Sullivan et al., 2003; Chen et al., 2004).

[1] These authors contributed equally to this work.
[2] To whom correspondence should be addressed. E-mail ilhalee@snu.ac.kr or xingwang.deng@yale.edu; fax 822-872-1993 or 203-432-3854.
The author responsible for distribution of materials integral to the findings presented in this article in accordance with the policy described in the Instructions for Authors (www.plantcell.org) is: Xing Wang Deng (xingwang.deng@yale.edu).
[W] Online version contains Web-only data.
www.plantcell.org/cgi/doi/10.1105/tpc.106.047688

Molecular genetic approaches have also revealed negative regulators of photomorphogenesis, designated CONSTITUTIVE PHOTOMORPHOGENIC/DEETIOLATED/FUSCA (COP/DET/FUS) (Sullivan et al., 2003; Wei and Deng, 2003). Recently, COP1 was shown to act as an E3 ubiquitin ligase for the degradation of two basic domain/leucine zipper (bZIP) transcription factors (HY5 and HYH), a MYB transcription factor (LAF1), and a basic helix-loop-helix (bHLH) transcription factor (HFR1), all of which are involved in promoting photomorphogenesis (Osterlund et al., 2000; Holm et al., 2002; Saijo et al., 2003; Seo et al., 2003; Jang et al., 2005; Yang et al., 2005).

HY5, a bZIP protein, is the first known and most extensively studied transcription factor involved in promoting photomorphogenesis. Mutations in *HY5* cause a defect in the inhibition of hypocotyl elongation in all light conditions, suggesting that HY5 acts downstream of phyA, phyB, cryptochromes, and UV-B (Koornneef et al., 1980; Oyama et al., 1997; Ang et al., 1998; Ulm et al., 2004). Therefore, HY5 is a pivotal transcription factor for photomorphogenesis that is regulated by multiple photoreceptors and the COP/DET/FUS protein degradation machinery. In addition, recent studies showed that the *hy5* mutant also has defects in root growth and hormone response (Oyama et al., 1997; Cluis et al., 2004), indicating that HY5 could act as a signal transducer that links hormone and light signaling, or that it plays additional roles beyond the light regulation of development. In vitro analysis showed that HY5 protein binds to the promoters of light-inducible genes such as *chalcone synthase* (*CHS*) and *ribulose bisphosphate carboxylase small subunit* (*RbcS1A*) (Ang et al., 1998; Chattopadhyay et al., 1998). However, it has not been demonstrated that those promoters are the in vivo binding targets of HY5.

Considering that HY5 plays such a pivotal role in plant developmental processes, it is of great importance to reveal the full range of HY5 target genes. Recently, a technique for genome-wide mapping of in vivo binding targets of a transcription factor was developed, which couples chromatin immunoprecipitation (ChIP) using an antibody specific to the transcription factor of interest and DNA chip hybridization with the DNA bound to chromatin as a probe (ChIP-chip) (Buck and Lieb, 2004; Euskirchen and Snyder, 2004). Because arrays representing the full genome of *Arabidopsis* have been developed, it is possible to monitor interactions between transcription factor and chromatin genome-wide in *Arabidopsis* (Yamada et al., 2003; Stolc et al., 2005; Thibaud-Nissen et al., 2006). In this study, using a microarray that represents almost all of the unique, nonrepetitive portion of the *Arabidopsis* genome, we performed genome-wide surveys of HY5 in vivo binding targets by ChIP-chip techniques. We found that HY5 binds to the promoters of a large number of genes that have diverse functions in plant growth and development.

RESULTS

ChIP with an Epitope-Tagged Transgenic Line

To map the binding sites of the HY5 transcription factor, we generated transgenic lines expressing hemagglutinin (HA)-tagged HY5. HA was chosen because the antibody for HA is commercially available and provides high specificity for immunoprecipitation and generic application for any transcription factors. The *35S-HA:HY5* (*HA:HY5* below) transgene completely rescued the phenotype of the *hy5* mutant, with hypocotyl length the same as the wild type in all light conditions tested (white, red, far-red, and blue light) (Figure 1A; data not shown). We selected the *HA:HY5* lines that possess HA:HY5 protein levels similar to endogenous HY5 (Figure 1B) for further analysis.

The previous in vitro analysis showed that HY5 protein binds to the promoters of *CHS* and *RbcS1A* (Ang et al., 1998; Chattopadhyay et al., 1998); thus, we used these two promoters as samples to check in vivo binding by ChIP followed by PCR. The ChIP-PCR assay was performed for the wild type and *HA:HY5* using HA-specific monoclonal antibody (Figure 1C). The promoters of *CHS* and *RbcS1A* were both enriched in *HA:HY5* seedlings relative to wild-type seedlings, which lacked HA:HY5 protein, whereas the negative control, the 3′ untranslated region of At4g26900 DNA, was not enriched by ChIP in the same samples. To determine whether such enrichment is HY5-specific, ChIP using HY5-specific antibody for the wild type compared with *hy5* was also performed. As shown in Figure 1D, the promoters of *CHS* and *RbcS1A*, but not At4g26900, were enriched in the wild type. These results confirm the in vivo binding of HY5 to the promoters of light-regulated genes and the feasibility of the epitope-tagging strategy for ChIP.

HY5 in Vivo Binding Activity Is Not Affected by Light

It was reported that HY5 acts downstream of multiple photoreceptors (Koornneef et al., 1980; Oyama et al., 1997; Ulm et al.,

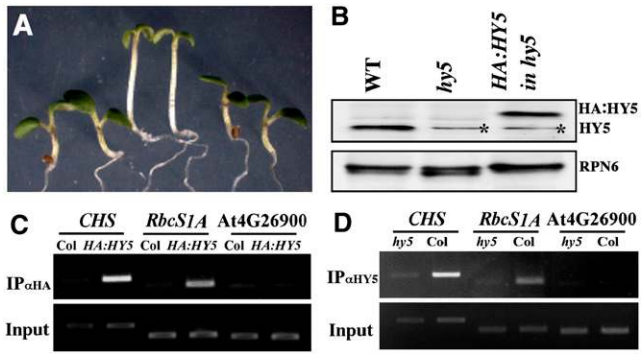

Figure 1. ChIP Confirms that HY5 Binds to the Promoters of *CHS* and *RbcS1A* in Vivo.

(A) The *HA:HY5* transgene complements the phenotype of the *hy5* mutant. Wild-type (left), *hy5* (middle), and *HA:HY5* in *hy5* (right) seedlings were grown under white light.

(B) The HA:HY5 protein amount in the *HA:HY5* transgenic line is similar to that of endogenous HY5 in the wild type. Total soluble protein extracts from 4-d-old white light–grown seedlings from each genotype were separated and immunoblotted with HY5-specific antibody (top) and RPN6-specific antibody (bottom). Asterisks indicate nonspecific cross-reacting protein. RPN6 shows the equal loading of proteins.

(C) ChIP with anti (α)-HA antibody for two positive controls, promoters of *CHS* and *RbcS1A*, and a negative control, At4g26900. Input control from nonimmunoprecipitated genomic DNA is shown at bottom. IP, immunoprecipitate.

(D) ChIP with αHY5 antibody. Input control is shown at bottom.

2004). We examined whether different qualities of light affect the in vivo binding activity of HY5 using the ChIP-PCR assay. The HA:HY5 abundance was not significantly different in 4-d-old seedlings grown under continuous white (Wc), Rc, or FRc light, whereas the amount was relatively low under blue light because of the low light intensity used (Figure 2A). In all light conditions, the promoters of *CHS* and *RbcS1A* were enriched in *HA:HY5* transgenic plants compared with wild-type plants, and the degree of enrichment was comparable among different light conditions (Figure 2B).

To test whether the HY5 in vivo binding activity is affected by the light-to-dark transition, we first checked the protein levels of HA:HY5 and endogenous HY5 in the transgenic line and the wild type, respectively, grown for 4 d under white light and then transferred to darkness, because HY5 protein is known to be degraded in the dark (Osterlund et al., 2000). As reported, the HY5 protein level was reduced relatively slowly but the HA:HY5 protein level was reduced very quickly in the dark, such that the half-life of endogenous HY5 was ~10 h but that of HA:HY5 was ~1 h (Figure 2C). We further examined whether HY5 proteins remain in the nucleus during the dark phase. Indeed, HY5 proteins were detected only in nuclear fractions and showed ~20% reduction after 8 h of darkness (Figure 2D). Because HA:HY5 was degraded faster than the endogenous HY5 during this light-to-dark transition, ChIP using HY5-specific antibody for endogenous HY5 was performed for wild-type and *hy5* mutant seedlings. The enrichment of the promoters of *CHS* and *RbcS1A* remained unchanged at 8 h after the dark transition, suggesting

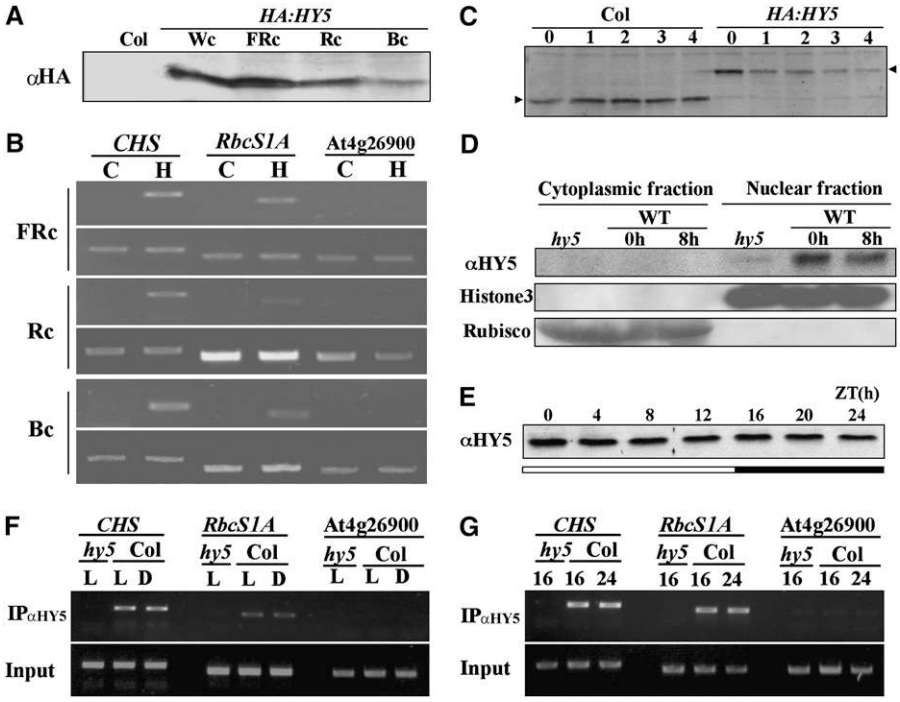

Figure 2. Effect of Light on HY5 in Vivo Binding Activity.

(A) HA:HY5 protein levels in different light conditions. *HA:HY5* was grown under Wc, Rc, FRc, or Bc for 4 d, and total protein extracts were separated and immunoblotted with anti (α)-HA antibody. Wild type (Col) grown under white light is shown as a control.

(B) ChIP with αHA antibody for the two promoters of *CHS* and *RbcS1A* and the negative control At4g26900. C indicates wild type; H indicates *HA:HY5*.

(C) Effect on HY5 protein levels of the light-to-dark transition. Wild-type and *HA:HY5* plants were grown under white light for 4 d, then transferred to dark. Total proteins were extracted at 1-h intervals after dark transfer. Arrowheads at left and right denote endogenous HY5 and HA:HY5 proteins, respectively. The half-life of HA:HY5 is ~1 h.

(D) HY5 proteins remain in the nucleus after the light-to-dark transition. Wild-type and *hy5* plants were grown under Wc light, then transferred to dark for 8 h. After nuclei isolation, proteins were extracted from the cytoplasmic fraction and the nuclear fraction. The purity of the nuclear fraction was demonstrated by specific antibody against histone 3, and the purity of the cytoplasmic fraction was demonstrated by Ponceau staining of ribulose-1, 5-bis-phosphate carboxylase/oxygenase (Rubisco) protein. Neither histone 3 nor HY5 is detected in the cytoplasmic fraction. After 8 h of transition to darkness, HY5 protein in the nuclear fraction is reduced by ~20%.

(E) The daily rhythm of endogenous HY5 protein level. Wild-type plants were grown under long days (16 h of light, 8 h of dark) for 4 d, then total protein was extracted every 4 h. The level of HY5 protein does not show significant diurnal change. ZT, Zeitgeber time.

(F) ChIP with αHY5 antibody for the promoters of *CHS* and *RbcS1A* and the negative control At4g26900. The *hy5* control and wild-type Columbia were grown under Wc light for 4 d (L), then half of the wild-type samples were transferred to dark conditions for 8 h of incubation (D). IP, immunoprecipitate.

(G) ChIP with αHY5 antibody for the promoters of *CHS* and *RbcS1A* and the negative control At4g26900. Wild-type plants were grown under long days for 4 d, then harvested at dusk (16 h after light on) and dawn (8 h after light off). The *hy5* control tissues were harvested at dusk with the wild-type tissues. Input control is shown at bottom.

that HY5 binding activity is not affected by transfer to darkness (Figure 2F). We also examined possible diurnal alterations of HY5 in vivo binding activity toward its targets. For this, wild-type seedlings were grown under a long-day cycle (16 h of light and 8 h of dark) for 4 d, then plant tissues were harvested at dusk (16 h after lights on) and the following dawn (8 h after the dark period) (Figure 2G). We observed that the expression of HY5 proteins did not show any significant diurnal change (Figure 2E) and that the level of enrichment in *CHS* and *RbcS1A* promoters was similar at dusk and dawn. This observation suggests that HY5 binding activity is not significantly affected by daily diurnal rhythms.

Genome-Wide HY5 Binding Site Analysis

To determine the in vivo HY5 binding sites in the *Arabidopsis* genome, four biological ChIP-chip replicate assays were performed using HA-specific antibody for *HA:HY5* lines. The DNA from each ChIP was labeled with Cy5 and the sonicated input DNA was labeled with Cy3, and the pooled probes were used for hybridization with 60mer probes on a microarray chip that covers the sequenced *Arabidopsis* genome (Figure 3A). The total gene number, including pseudogenes, in *Arabidopsis* is 30,700 based on Arabidopsis Genome Initiative genome version 5 (December 10, 2004), and the total oligonucleotides spotted on the microarray chip was 193,751, with one oligonucleotide covering every 500 ± 25 nucleotides throughout the genome (Figure 3). On average, our microarray contains ~6.3 oligonucleotides for each gene.

From the analysis of ChIP-chips, 3894 genes were selected as putative HY5 binding target genes that were distributed over all five chromosomes (Figure 3B). Among them, the annotated pseudogenes were selectively depleted, because only 2.1% of pseudogenes (80 among 3786 pseudogenes) were identified as targets compared with 14.5% of normal genes (3894 among 26,914 genes). To evaluate the ChIP-chip results, the frequency of false-positives was determined by conventional ChIP-PCR using 18 randomly selected target genes based on ChIP-chip data (see Supplemental Figure 1 online). All genes (18 of 18) that we checked showed enrichment by this ChIP-PCR assay. Furthermore, ChIP-PCR analysis of 12 additional target genes from specific functional groups validated 11 of them (see Supplemental Figures 2 and 3 and Supplemental Table 2 online; see below). It is worth noting that the validation ChIP-PCR experiments were done using both HA:HY5 and endogenous HY5 and the results were always the same, indicating that the epitope-tagged HA:HY5 protein worked like the endogenous HY5 for ChIP-chip. Therefore, most of the putative HY5 binding target genes determined by ChIP-chip are likely to be HY5 binding targets, and we refer to them herein as HY5 target genes.

The relative positions of oligonucleotides enriched by HY5 showed that 61.3% of them were located on the intergenic regions, where either one or both promoters of neighboring genes reside, indicating that HY5 preferentially binds to the promoters (Figure 3C). The frequency of enriched oligonucleotides located on the proximal downstream side of the translational start codon ATG (<500 bp downstream) also was enriched significantly compared with the whole genome. By contrast, the frequency on the distal downstream side of the start codon (>500 bp downstream) and convergent intergenic regions was depleted significantly compared with the whole genome. Considering that the average size of DNA fragments sheared by sonication before immunoprecipitation was ~400 to 600 bp and, thus, ~500 bp upstream or downstream of real binding sites can be enriched, our results suggest that the promoter regions are preferentially enriched by HY5. The distribution of relative frequency of HY5 binding sites over various parts of the gene structure (Figure 3D) also supports the notion that HY5 preferentially binds to the promoter regions.

The binding site–searching software MDscan and Weeder failed to discover novel motifs within the 2-kb upstream region of HY5 target genes except the known G box, Z box, and its variants. When those known consensus binding sites of HY5 were searched in the promoter regions of HY5 target genes, the frequency of the G box (CACGTG) was highest, and it was ~1.6 times higher in the target genes compared with the whole genome. In addition to G box, CG hybrid (GACGTG) and CA hybrid (GACGTA), that are also known as HY5 binding consensus sequences (Hong et al., 2003), and Z box, that is known as one of the light-responsive elements, showed higher frequency in the target genes than in the whole genome (Figure 3E).

The Functional Classification of HY5 Targets

The functional classification of HY5 targets based on gene ontology showed that HY5 binds to a wide range of genes with diverse functions (Figure 4). The genes encoding proteins involved in metabolism, energy, transcription, cellular transport, biogenesis of cellular components, subcellular localization, and photosynthesis showed statistically higher frequency in HY5 target genes than in the whole genome. Interestingly, the frequency of transcription factors among HY5 targets was ~1.6 times higher than that found within the whole genome (Figure 4). The genes encoding transcription factors among HY5 targets included nine *AUX/IAA*s, six *AUXIN RESPONSE FACTOR*s, six *ERF*s (for *ETHYLENE-RESPONSIVE FACTOR*), and two *REPRESSOR OF GA1*s, which mediate hormone signaling (see Supplemental Table 1 online for the whole list of HY5 targets). HY5 target genes also included light-signaling components (*HFR1*, *PIF4*, *HYH*, and *PKS1*), flowering time regulators such as *SOC1*, *GI*, and *FRI*, and circadian rhythm regulatory components (see Supplemental Table 1 online).

Comparison of ChIP-Chip with Genome-Wide Expression Analysis

To determine the functional relevance of the HY5 binding sites to the transcriptional regulation, we performed genome-wide expression analysis using wild-type and *hy5* plants grown in Wc light for 4 d, the same conditions used for ChIP-chip assays. For this analysis, we used a 70mer oligonucleotide microarray that covers 25,676 unique genes (Ma et al., 2005). From four biological replicate experiments, 1144 genes were differentially expressed by twofold or greater with $P < 0.05$. Among them, 594 genes were downregulated and 550 genes were upregulated in *hy5*. The comparison with HY5 binding targets showed that ~26% of the downregulated genes and 12% of the upregulated genes in *hy5* were HY5 binding targets (Figure 5, Table 1). In total, 19% of the

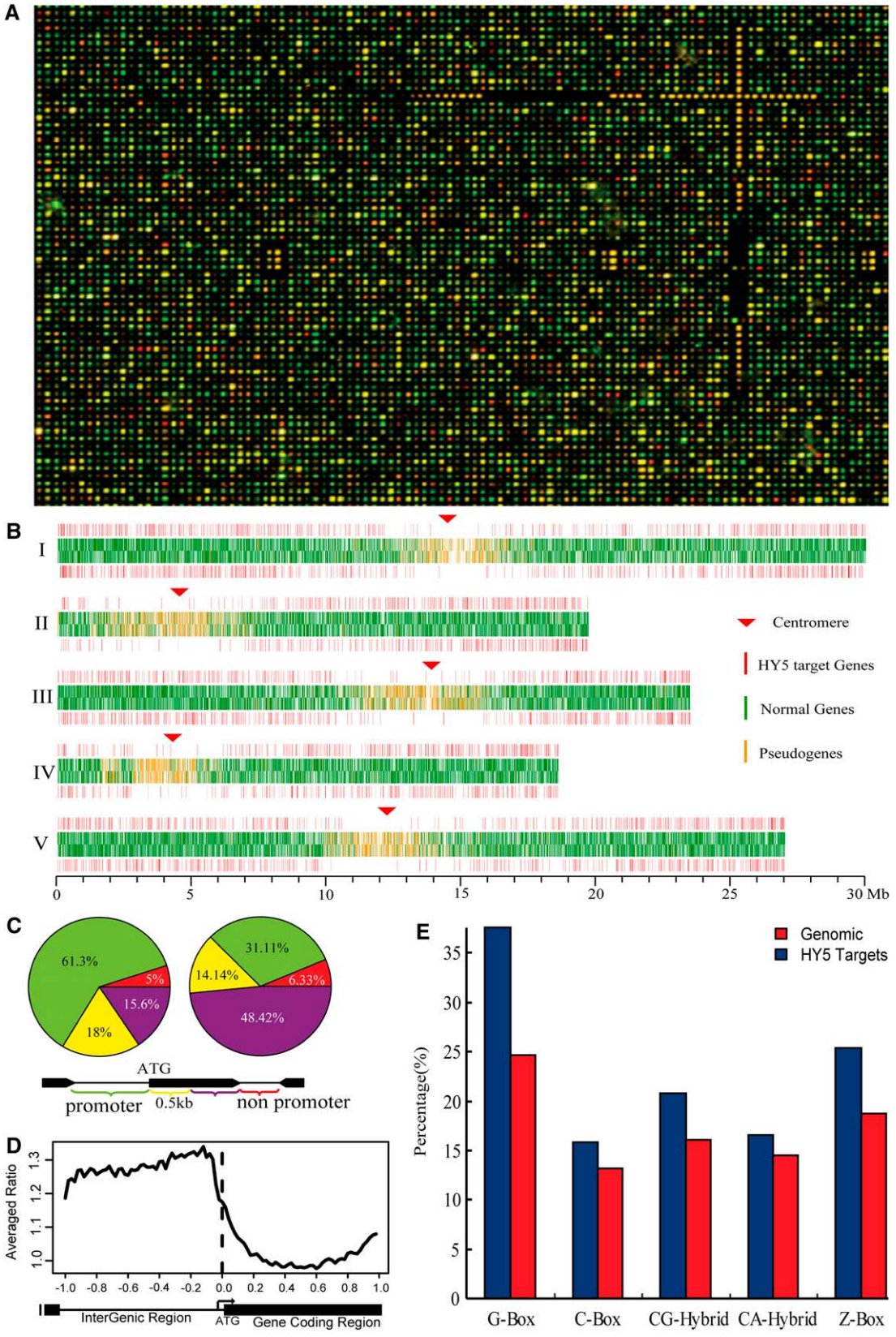

Figure 3. Overview of Genome-Wide HY5 Binding Analysis.

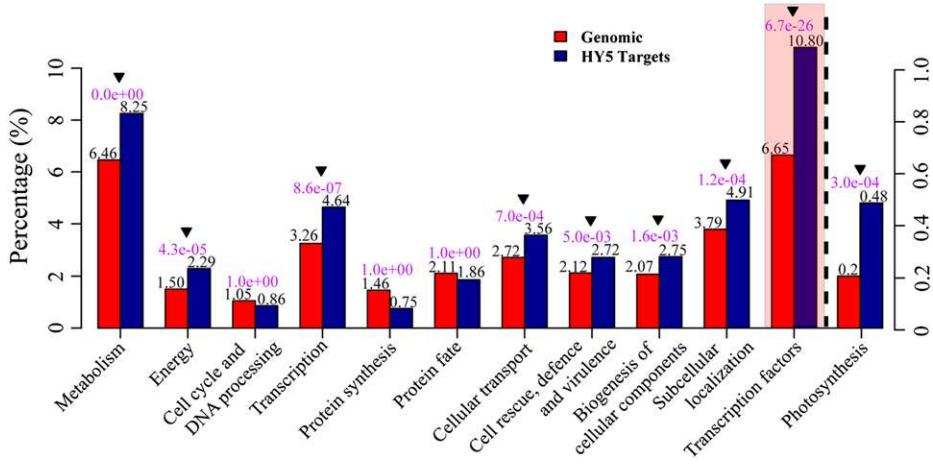

Figure 4. Functional Classification of the HY5 Binding Target Genes.

Part of the top functional categories of HY5 target genes using the Munich Information Center for Protein Sequences FunCat website. Transcription factors were identified based on the Database of Arabidopsis Transcription Factors and are indicated with a pink background. At right of the dotted line is the photosynthesis subcategory, shown on a different scale. The percentage of each category is compared with the whole genome, and hypergeometric test P values are shown above the bars. Arrowheads indicate significantly different categories ($P < 0.01$).

differentially expressed genes were included in HY5 binding targets, indicating that they were regulated directly by HY5.

It is interesting that our HY5 target collection correlates with HY5-coexpressed genes described in a previous report (Obayashi et al., 2004). In that report, the authors evaluated the relative expression values of 8809 genes. Among their top 30 HY5 coexpression genes, 28 (93%) are included in our HY5 target genes list. The two remaining genes, At5g17050 (UDP-glucuronosyl/UDP-glucosyl transferase family protein) and At3g29200 (chorismate mutase, chloroplast), have HY5 binding signal just below our target gene selection criteria (see Methods). Because it is anticipated that the direct target genes of HY5 would tend to exhibit a similar expression pattern as HY5, this observed degree of enrichment of the HY5 coexpressed genes among the HY5 target gene group substantiates this notion.

Comparison of the HY5 Binding Sites with Light-Regulated Gene Profiles

Because HY5 protein mediates far-red, red, blue, and even UV-B light signaling, we hypothesized that many of the HY5 binding sites would overlap with light-regulated genes; thus, we compared our HY5 binding targets with the light-regulated gene profiles reported previously.

First, we compared organ-specific expression profiles that are regulated by light (Ma et al., 2005). From cotyledon, hypocotyl, and root tissues analyzed, 3103 genes were differentially expressed greater than twofold by light (Ma et al., 2005). Our comparison showed that ~24% of them (738 genes) had the HY5 binding sites in their promoters (Figure 6A). Compared with gene expression profiles from individual organs, a similar proportion of genes had HY5 binding sites irrespective of organs (Figure 6B). In addition, the proportions of HY5 binding targets among light-induced genes and light-repressed genes were not much different in cotyledon and hypocotyl, although the proportion was slightly higher among light-induced genes than light-repressed genes in root (Figures 6B and 6C). Although HY5 is well known as a positive regulator of light signaling, the data here indicate that HY5 acts as both an activator and a repressor for transcriptional regulation (Figure 6D). Our results also suggest that HY5 contributes to the light regulation of genome expression to a similar extent in each organ.

Figure 3. (continued).

(A) A representative microarray hybridization result showing part of the chip. Only a 1/400th area of the chip is shown. The images of Cy5 (red) for enriched DNA by HY5 and Cy3 (green) for input genomic control DNA are merged.

(B) Distribution of HY5 target genes throughout the five chromosomes of *Arabidopsis*. The two top bars are for genes oriented 5′ to 3′, and the two bottom bars are for genes oriented 3′ to 5′. The putative HY5 target genes are depicted in red bars at the uppermost and lowermost positions. For the two middle bars, normal genes are depicted in green and pseudogenes are depicted in yellow.

(C) The distribution of the positions of HY5 binding sites (left) relative to the gene structure was compared with the whole genome (right). A scheme illustrating each position of a binding site in relation to a transcription unit is shown at bottom. The percentages of binding sites at each position are shown.

(D) Frequency of HY5 binding sites (as viewed through the averaged ratio of ChIP hybridization signal to the total genomic control) along the virtually normalized gene models of the whole *Arabidopsis* genome.

(E) Percentage of putative target genes in which promoters contain HY5 binding consensus sites—G box, C box, CG hybrid, CA hybrid, and Z box—compared with the whole genome.

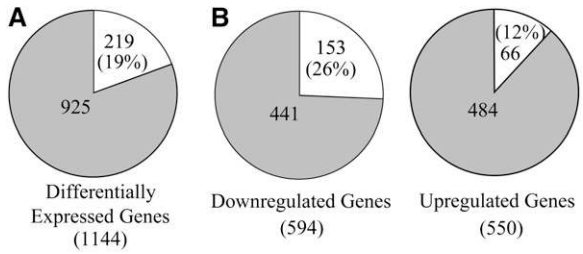

Figure 5. Comparison of ChIP-Chip Data with Genome-Wide Expression Analysis.

(A) Experimental expression analysis of the *hy5-221* mutant compared with Columbia wild type. A 2.7K 70mer microarray was used in this analysis. The total number represents the number of differentially expressed genes by twofold or greater ($P < 0.05$) in *hy5-221*. The white area represents the number of differentially expressed genes that also have HY5 binding sites and their percentage compared with total differentially expressed genes.

(B) Relative proportion of upregulated and downregulated genes in *hy5* that also have HY5 binding sites.

We also compared the HY5 binding target genes with the phyA- and phyB-regulated gene expression profiles obtained with the 8.2K Affymetrix chip (Tepperman et al., 2001, 2004). Tepperman et al. (2001, 2004) obtained gene expression profiles after 1 and 24 h of FRc and Rc irradiation in a phyA- or phyB-dependent manner. They defined the differentially expressed genes as early-regulated genes (at 1 h) and late-regulated genes (at 24 h). Overall, 34% of the genes induced by FRc, 34% of the genes repressed by FRc, 33% of the genes induced by Rc, and 32% of the genes repressed by Rc were HY5 binding targets (Figure 7A). Thus, similar proportions of genes among phyA- and phyB-regulated genes are HY5 binding targets. This also confirms that HY5 acts both for transcriptional activation and transcriptional repression.

When we compared HY5 binding targets with early-regulated genes and late-regulated genes separately, the proportion of HY5 binding targets was approximately twice in early-induced genes than in late-induced genes. That is, 60% (FRc) and 60% (Rc) of the early-induced genes by light were HY5 binding targets, whereas 31% (FR) and 27% (R) of the late-induced genes were HY5 binding targets (Figure 7B; see Supplemental Table 3 online). This indicates that HY5 preferentially mediates an early event of phyA- and phyB-regulated gene expression. In addition, the proportion of transcription factors among HY5 targets was significantly higher than among non-HY5 targets in early-induced genes (Figures 7C and 7D). Together, our analyses strongly suggest that HY5 plays an important role in the early phase of phytochome A– and B–mediated light control of gene expression.

Direct Regulation of Photosynthesis-Related Genes by HY5

Functional classification of HY5 targets showed that the photosynthesis-related genes were the most highly enriched group compared with the whole genome (Figure 4). Therefore, we investigated whether HY5 directly regulates such genes (Figure 8). *CAB1* (encoding chlorophyll *a/b* binding protein1), *F3H* (encoding flavanone 3′ hydroxylase), as well as *CHS* and *RbcS1A*, which have functions in chlorophyll and anthocyanin biosynthesis, showed enrichment, as confirmed by ChIP-PCR (Figure 8A). This result was also confirmed by quantitative real-time PCR (Figure 8B). When the 4-d-old dark-grown seedlings were transferred to white light, the accumulation rate of chlorophyll and anthocyanin contents was slower in the *hy5* mutant than in the wild type (Figure 8E). Consistently, the extent of induction of these genes was reduced in *hy5* compared with the wild type during dark-to-light transitions (Figure 8C), and the expression of *F3H* was much lower in the *hy5* mutant compared with the wild type in constant light (Figure 8D). This result supports the conclusion that HY5 directly regulates the transcription of photosynthesis-related genes during seedling photomorphogenic development.

HY5 Binding to Promoters of Circadian Regulator Genes

To our surprise, many genes involved in the regulation of circadian rhythms were included in the collection of HY5 binding target genes (see Supplemental Table 1 online). The ChIP-PCR analysis confirmed the enrichment of promoter regions of several circadian regulators (see Supplemental Figure 2 online). Thus, we examined the effect of *hy5* and the light-to-dark transition on the expression of the circadian regulators. As shown in Figure 9, the expression levels of *CCA1*, *LHY*, *TOC1*, *ELF3*, *GI*, and *FKF1* were not significantly changed by either the *hy5* mutation or the 8-h light-to-dark transition. By contrast, the randomly selected HY5 binding target genes among those downregulated in *hy5* (analyzed in Figure 5) showed decreases in expression by both *hy5* and dark transition (Figure 9). They are At5g52020, At2g35930, At5g02270, At5g44110, and *MYB12*. Consistent with the minimal effect of *hy5* on the expression of circadian regulators, the effect of *hy5* on the circadian rhythm was very subtle (data not shown) (Anderson et al., 1997; Hicks et al., 2001). This was also consistent with the constant HY5 binding to the promoters of the circadian regulators during the light-to-dark cycle in long days (see Supplemental Figure 3 online). Together with the fact that HY5 binds to the promoter regions of both morning-expressed oscillator (*CCA1/LHY*) and evening-expressed oscillator (*TOC1/ELF4*), our results imply that HY5 binding alone is not sufficient to maintain the proper circadian rhythm and likely works with other factors redundantly.

DISCUSSION

In this study, we report a reliable method to analyze the in vivo binding sites of HY5 and verify several of its suspected target promoters. The genome-wide searching of in vivo binding targets showed that HY5 preferentially binds to promoters, although a small fraction of binding sites is located at other regions of genes. The putative HY5 binding sites were mapped to 3894 genes that have diverse functions in plant growth and development. Approximately 10% of the HY5 target genes were transcription factors, which is something of an overrepresentation compared with the whole genome. This observation supports the idea that HY5 is a higher hierarchical regulator of the transcriptional cascade for photomorphogenesis.

Table 1. List of Representative HY5 Binding Targets That Are Differentially Expressed in a *hy5* Mutant

Genes Positively Regulated by HY5			
At5g65260	Polyadenylate binding protein family protein/PABP family	At1g18300	At NUDT4, Nudix hydrolase homologues, cytosol
At5g60360	Cys-type endopeptidase activity, proteolysis/AALP protein	At5g47590	Unknown
At5g13930	*CHS*, chalcone synthase, regulation of anthocyanin biosynthesis	At3g62260	Protein phosphatase type 2C, chloroplast
At5g10100	Trehalose-phosphatase activity	At2g25460	Unknown
At5g08640	*FLS*, flavonoid biosynthesis	At1g18740	Unknown
At5g44110	*POP1*, transporter activity	At3g50800	N-terminal protein myristoylation
At1g19210	Transcription factor	At1g77640	Transcription factor
At1g66160	Ubiquitin ligase activity	At5g25810	TINY transcription factor, AP2 domain
At1g24140	Proteolysis, metalloendopeptidase activity	At2g22880	Unknown, choloroplast
At1g09480	Lignin biosynthesis, cinnamyl-alcohol dehydrogenase activity	At1g68840	Transcription factor
At4g32800	Transcription factor	At1g56660	Unknown
At1g59640	Transcription factor	At5g57510	Unknown, mitochondrion
At4g37770	ACS8, ethylene biosynthesis	At1g76600	N-terminal protein myristoylation, nucleus
At1g80850	DNA repair, DNA–3-methyladenine glycosylase I activity	At3g50850	Unknown
At5g01730	Unknown	At1g68620	Unknown
At5g41170	Unknown	At3g46080	Transcription factor zinc ion binding
At4g34410	Transcription factor	At2g28630	Acyltransferase activity, endomembrane system
At1g33560	ADR1, kinase, defense response	At2g33580	Cell wall catabolism, kinase activity
At5g49520	WRKY transcription factor	At2g35290	Unknown, mitochondrion
At1g76650	Chloroplast protein, calcium ion binding protein	At2g34330	Chloroplast
At4g31870	ATGPX7, oxidative stress	At1g61340	Unknown, mitochondrion
At3g51240	F3H, flavonoid biosynthesis	At2g35930	Ubiquitin ligase activity
At3g02840	Response to pathogen	At5g52020	Transcription activator
At5g03210	Unknown	At5g54510	DFL1, cell growth, auxin-mediated signaling pathway
At3g55240	Unknown	At5g65300	Chloroplast
At5g05270	Flavonoid biosynthesis	At3g55980	Transcription factor
At4g29780	Unknown	At5g67400	Peroxidase
At1g17420	Lipoxygenase, JA biosynthesis	At5g59550	Zinc ion binding, protein binding
At1g73540	Hydrolase, chloroplast	At5g23010	MAM1, 2-soprophymalate synthase activity
At4g27280	Chloroplast protein, calcium ion binding protein	At4g13010	Oxidoreductase, thylakoid membrane
At1g25400	Unknown	At5g15510	Unknown
At5g02270	ATNAP9, transporter activity	At2g47460	MYB12
At5g62520	SRO5,oxygen and reactive oxygen species metabolism	At3g54810	BME3-ZF, GATA-type zinc finger,
At2g37430	Transcription factor zinc ion binding	At1g61890	Antiporter activity
At2g30040	Protein Tyr kinase activity, protein Ser-Thr kinase	At4g34150	Rhodopsin-like receptor, response to cold
At5g43890	Monooxygenase, auxin biosynthesis	At5g66210	Calcium- and calmodulin-dependent protein kinase activity
At1g19380	Unknown	At5g02280	Endoplasmic reticulum to Golgi vesicle-mediated transport
At2g36220	Unknown	At2g32510	Protein-Tyr kinase activity
At2g22500	Mitochondrial transport	At5g01100	Unknown, choloroplast
At3g01830	Calcium binding	At4g33920	Protein phosphatase type 2C, mitochondrion
At1g73500	Mitogen-activated protein kinase kinase	At2g03300	Transmembrane receptor, defense response
At2g44080	Unknown	At5g05410	DREB2A, response to water deprivation and UV-B
At2g41640	Unknown	At1g60190	Ubiquitin–protein ligase activity
At3g13600	Unknown	At2g39650	Unknown

(Continued)

Table 1. (continued).

Genes Positively Regulated by HY5			
At3g48520	Monooxygenase, electron transport	At4g36670	Carbohydrate transporter
At5g62180	Catalytic activity	At3g09010	Tyr protein kinase, Ser/Thr kinase activity
At5g59820	RHL41, transcription factor, response to abiotic stress	At3g61680	Triacylglycerol lipase activity
At5g45110	Protein binding	At3g62720	Transferase activity, transferring glycosyl groups
At4g25490	CBF1, response to cold	At3g52400	SYP122, secretion, cell wall deposition
At4g27250	Cinnamyl-alcohol dehydrogenase activity	At3g25250	AGC kinase
At5g01550	Protein kinase	At4g27310	Heterotrimeric G-protein complex
At5g50950	Fumarate hydratase activity	At2g37530	Transferase activity
At3g06160	Transcription factor	At1g78990	Unknown
At4g08950	Unknown, cell wall	At3g23610	Protein Tyr/Ser/Thr phosphatase activity
At4g05100	At MYB74, response to JA, ABA, and ethylene	At5g64550	Unknown
At3g22830	Transcription factor	At5g13700	Oxidoreductase, electron transport
At2g29670	RNA processing	At5g51190	Transcription factor
At2g34990	Protein binding	At5g45820	CIPK20, Ser/Thr kinase, response to ABA
At3g05820	β-Fructofuranosidase activity	At1g53170	AP2/EREBPs (ethylene-responsive element binding proteins) transcription factor
At2g41100	TCH3, calmodulin-related proteins	At4g36040	Heat shock protein binding, chloroplast
At5g64660	Ubiquitin–protein ligase activity	At5g62020	Transcription factor
At3g52740	Unknown	At3g19350	Unknown
At4g17500	At ERF1(ethylene-responsive element binding factor)	At5g45630	Unknown
At5g66650	Unknown, mitochondrion	At5g49280	Unknown, membrane
At2g02870	Unknown	At3g60550	Cyclin-dependent protein kinase activity
At1g57770	Flavin adenine dinucleotide binding, carotinoid biosynthesis, oxidoreductase	At1g71697	At CK1, choline kinase activity
At3g56880	Unknown	At3g17130	Pectinesterase inhibitor activity
At2g27080	Unknown	At2g42870	Unknown
At5g53310	Unknown	At5g45340	CYP707A3, monooxygenase, ABA catabolism
At1g78440	Gibberellin 2-β-dioxygenase activity	At4g21420	Gypsy-like retrotransposon family
At3g14440	NCED3, 9-*cis*-epoxycarotenoid dioxygenase activity, ABA synthesis	At3g19350	Polyadenylate binding protein–related
At1g02810	Pectinesterase family protein	At1g17380	Unknown
At1g07135	Unknown	At1g18570	Myb family transcription factor (MYB51)
At1g09070	SRC2 involved in protein storage vacuole targeting	At1g19180	Unknown
At1g12950	MATE efflux family protein	At1g20510	4-Coumarate–CoA ligase family protein
At1g21910	DREB subfamily A-5 of ERF/AP2 transcription factor family	At1g22750	Expressed protein
At1g35720	Encodes a member of the annexin gene family		
Genes Negatively Regulated by HY5			
At1g32450	Proton-dependent oligopeptide transport (POT) family protein	At2g27660	DC1 domain–containing protein
At5g45850	Unknown	At2g43590	Chitinase, similar to basic endochitinase CHB4 precursor
At1g10760	SEX1, starch catabolism, α-glucan, water dikinase activity	At5g01300	Phosphatidylethanolamine binding family protein
At5g07680	No apical meristem (NAM) family protein, similar to CUC2	At2g15020	Expressed protein
At4g01610	Cys-type endopeptidase activity	At4g37070	Patatin, putative, similar to patatin-like latex allergen
At5g17760	Nucleoside-triphosphatase activity	At3g06080	Unknown
At4g15230	ATPase activity	At4g36030	Unknown
At3g01350	Proton-dependent oligopeptide transport (POT) family protein	At2g25890	Sequestering of lipid, membrane

(Continued)

Table 1. (continued).

Genes Negatively Regulated by HY5			
At1g15380	Lactoylglutathione lyase activity	At5g24140	Sterol biosynthesis, oxidoreductase activity
At1g55550	Microtubule motor activity, kinesin motor protein–related	At3g04140	Unknown, protein binding
At1g78850	Curculin-like (mannose binding) lectin family protein	At1g80130	Unknown, chloroplast
At1g16850	Unknown	At2g41850	Polygalacturonase activity, endomembrane system
At1g78390	NCED9, 9-*cis*-epoxycarotenoid dioxygenase, biosynthesis of ABA	At1g69760	Unknown
At2g43050	Pectinesterase family protein, cell wall modification	At5g62490	Unknown
At4g34610	BLH6, homeodomain, similar to homeotic protein BEL1	At2g29630	Thyamine biosynthesis, chloroplast
At5g55220	Peptidyl-prolyl *cis-trans*–isomerase	At2g28780	Unknown, mitochondrion
At3g16910	Acetate-CoA ligase activity	At1g63190	Unknown
At5g59930	DC1 domain–containing protein/UV-B light–insensitive	At2g31980	Cys protease inhibitor activity, endomembrane
At3g07650	COL9, negative regulation of photoperiodism, flowering	At2g33380	RD20, response to salt stress, ABA, desiccation
At5g55620	Unknown	At4g37230	Oxygen-evolving enhancer protein, chloroplast
At2g46660	Cytochrome P450, putative, similar to cytochrome P450 (CYP78A9)	At3g15670	Late embryogenesis–abundant protein, putative
At2g38750	Annexin 4 (ANN4), nearly identical to annexin (AnnAt4)	At3g21720	Isocitrate lyase, glyoxylate cycle
At5g59780	MYB59, response to GA, JA, salt stress, ABA, ethylene, and auxin	At5g44120	12S seed storage protein (CRA1)
At1g62780	Unknown, chloroplast	At2g35300	Late embryogenesis–abundant group 1 domain–containing protein
At4g32190	Chloroplast	At3g03450	RGL2, transcription factor, negative regulation of GA signaling
At1g17460	TRFL3, Myb-like DNA binding domain	At1g72100	Late embryogenesis–abundant group 1 domain–containing protein
At2g41670	GTP binding family protein	At4g35030	Protein kinase
At2g05160	Zinc finger (CCCH-type) family protein/ RRM-containing protein	At3g02990	Heat shock transcription factor 2 (HSTF2), identical to HSF2
At2g40170	Em-like protein GEA6 (EM6), Em-like protein GEA6	At2g43570	Chitinase, putative, similar to chitinase class IV
At1g27480	Lecithin:cholesterol acyltransferase family protein/LCAT family	At3g21890	Zinc finger (B box type) family
At5g53370	Pectinesterase family protein	At3g42930	CACTA-like transposase family
At1g03630	PORC, NADPH dehydrogenase activity	At1g24530	Transducin family protein/WD-40 repeat family protein
At1g13600	bZIP transcription factor family protein	At1g17100	SOUL heme binding family protein

ABA, abscisic acid; JA, jasmonic acid.

ChIP-Chip Analysis Reveals a Large Number of HY5 Target Sites in the *Arabidopsis* Genome in Vivo

The technique of ChIP-chip for genome-wide analyses of transcription factor binding sites has been applied successfully in yeast, which has a relatively small genome size (Buck and Lieb, 2004). Although this technique has also been applied in mammalian systems, only part of the genome rather than the whole genome was analyzed using either biased DNA arrays, such as those containing only sequences proximal to the promoter, or unbiased DNA arrays, which include only a couple of chromosomes (Martone et al., 2003; Cawley et al., 2004; Euskirchen et al., 2004). Here, we present a transcription factor binding site analysis at the whole genome scale in *Arabidopsis*, which was also reported independently by another laboratory recently (Thibaud-Nissen et al., 2006). Using a high-density 60-nucleotide oligomer microarray covering the entire *Arabidopsis* genome, we mapped genome-wide in vivo HY5 binding sites. First, our ChIP-PCR and ChIP-chip analyses proved that the putative binding targets of HY5, the promoters of *RbcS1A* and *CHS*, which were suggested by in vitro analysis, were indeed in vivo binding targets. Second, when 18 randomly selected genes from the ChIP-chip–positive pool were examined via ChIP-PCR, none

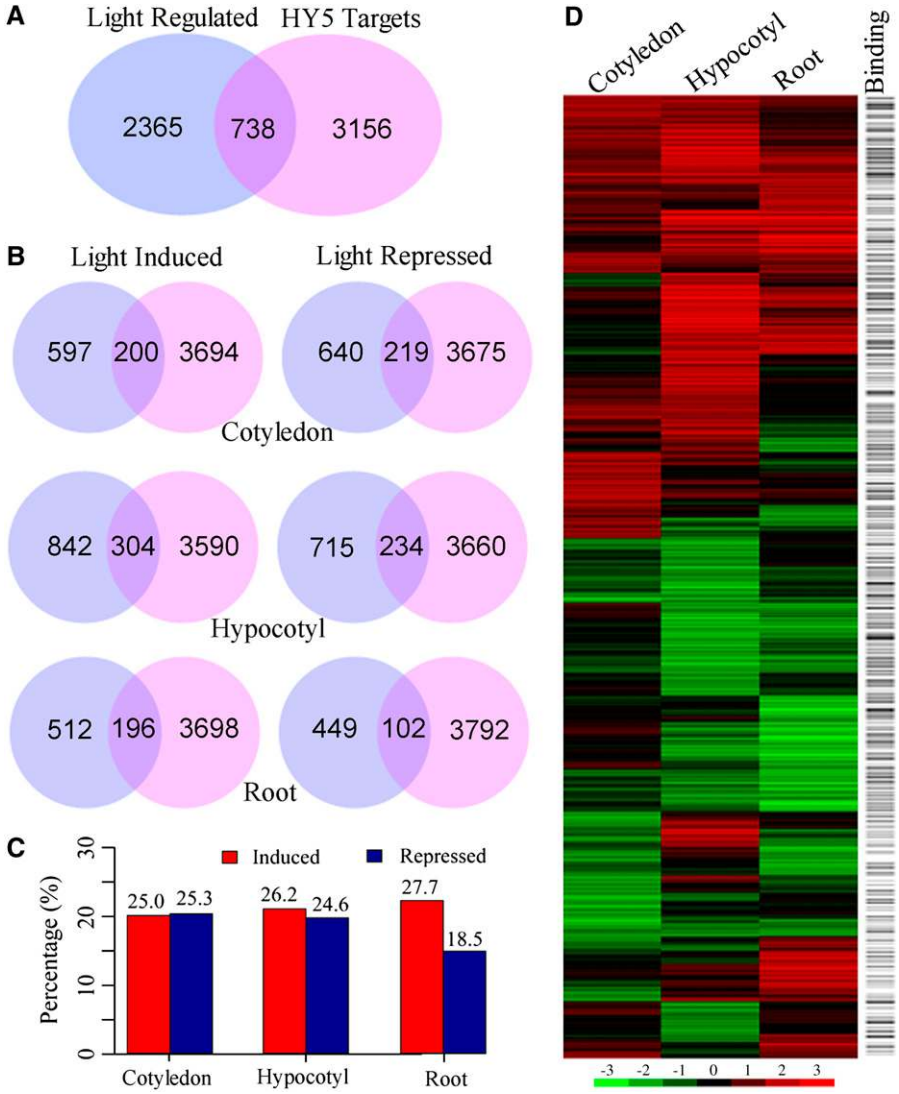

Figure 6. Comparison of ChIP-Chip Data with Organ-Specific Expression Profiles That Are Regulated by Light.

(A) Venn diagram of the differentially expressed gene profiles in all tissues (cotyledon, hypocotyl, and root) (Ma et al., 2005) and ChIP-chip data. Numbers in the overlapping areas indicate the number of genes that exhibited twofold or greater differential expression in each organ and that have HY5 binding sites in their promoters.

(B) Venn diagram of the differentially expressed (at least twofold at $P < 0.05$) gene profiles in all tissues (cotyledon, hypocotyl, and root) and ChIP-chip data. At left is a comparison of genes upregulated by light and HY5 binding targets, and at right is a comparison of genes downregulated by light and HY5 binding targets.

(C) Percentage of HY5 binding targets among the genes expressed differentially by light in each organ analyzed in **(B)**.

(D) Hierarchical clustering display of white light–regulated genome expression among the three seedling organs. Horizontal black lines denote the presence of HY5 binding sites.

was false-positive. Furthermore, 11 of 12 putative genes from functional groups of interest were also verified. Third, the frequency of HY5 binding sites located on the pseudogenes was very low, suggesting a correlation with transcriptional regulation. Fourth, unbiased in vivo mapping in the *Arabidopsis* genome showed that HY5 preferentially binds to intergenic regions where promoters are located. Fifth, >70% of HY5 target genes obtained by ChIP-chip have HY5 binding consensus sequences as G box, C box, CG hybrid, and CA hybrid in the promoters (Figure 3E). Finally, we show that the HY5 binding to the promoters of some photosynthesis-related genes indeed is required for transcriptional regulation. Therefore, our results demonstrate that the ChIP-chip technique developed here is a valid approach for transcription factor target analysis in *Arabidopsis*.

Compared with the much smaller number (51) of putative binding sites of transcription factor TGA2 identified recently in a

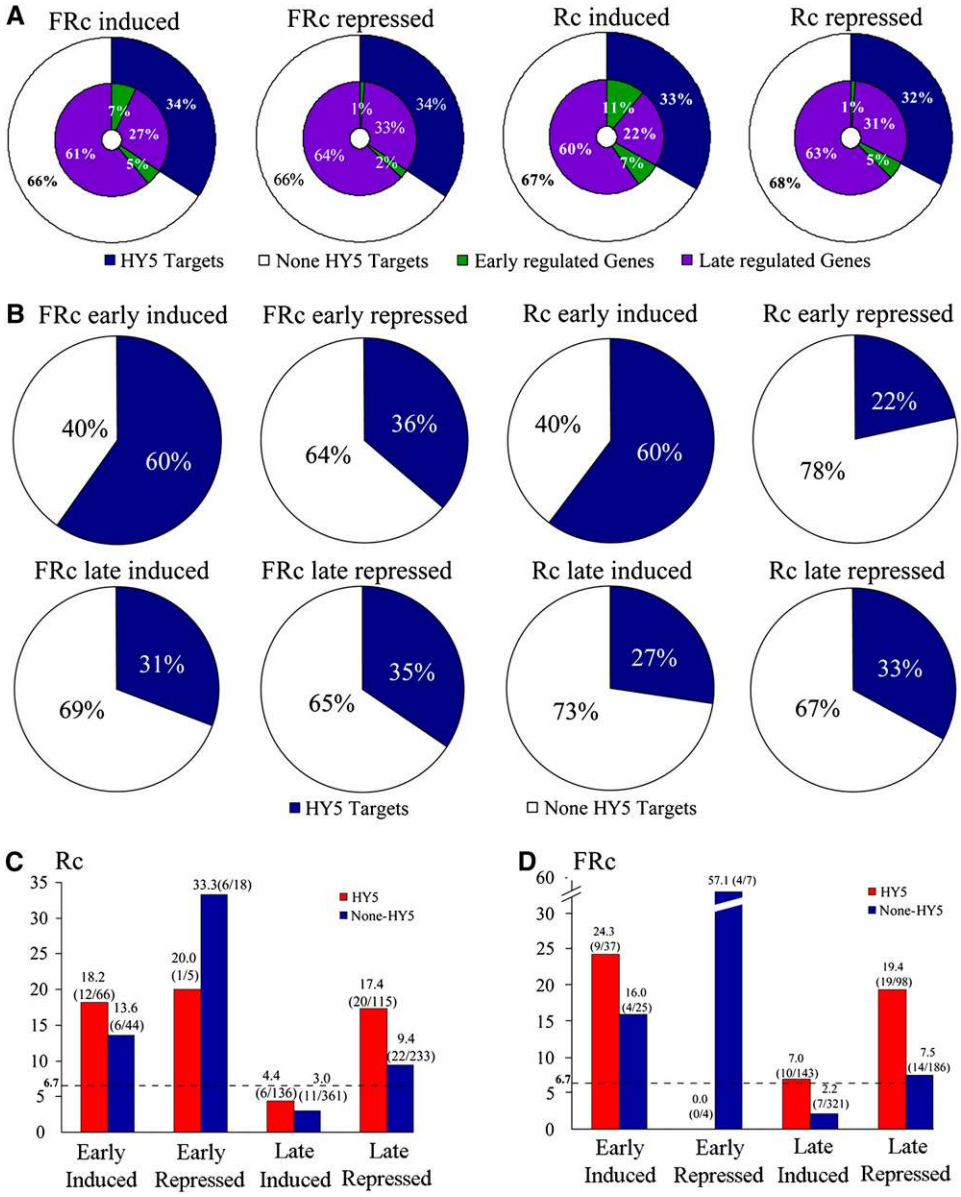

Figure 7. Comparison of the HY5 Binding Target Genes with the phyA- and phyB-Regulated Gene Expression Profiles Using the 8.2K Affymetrix Chip (Tepperman et al., 2001, 2004).

(A) The percentage of HY5 binding targets is shown in dark blue in each gene group.
(B) The percentage of HY5 binding targets in each subgroup is shown in dark blue in each circle.
(C) and **(D)** The numbers of transcription factors of each subgroup are shown for Rc light–regulated **(C)** and FRc light–regulated **(D)**.

similar ChIP-chip assay (Thibaud-Nissen et al., 2006), we identified ~3800 putative in vivo binding targets for HY5. Although this number is larger than anticipated, similar cases were also observed for other transcription factors in human ChIP-chip research (Cawley et al., 2004). Cawley et al. (2004) predicted many more cMyc (25,000) and Sp1 (12,000) putative binding sites than p53 (1600) binding sites in the whole genome based on a survey of human chromosomes 21 and 22 using the same tiling array designs. Those findings suggest that different transcription factors tend to have different pool sizes of binding sites according to how they function in downstream events.

Previously, a 3.8K promoter chip was developed in our group to map the HY5 binding sites by in vitro binding analysis using glutathione *S*-transferase–HY5 (Gao et al., 2004). In comparing in vivo binding targets obtained here by the ChIP-chip technique and the in vitro binding analysis using the 3.8K promoter chip, we found a very low degree of overlap between the two data sets. Only 2 of 42 genes that were proposed as HY5 binding candidates

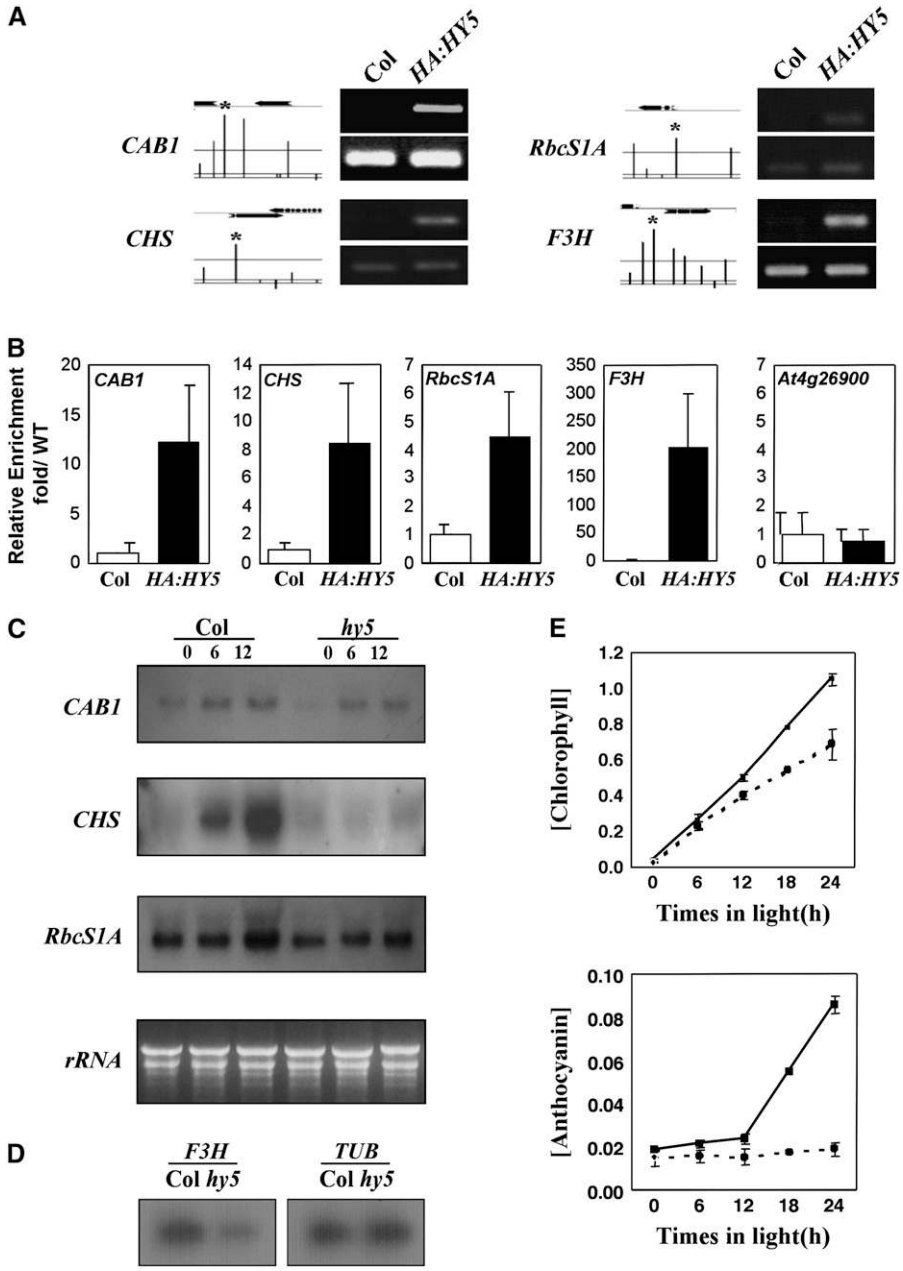

Figure 8. HY5 Directly Regulates Photosynthesis-Related Genes.

(A) ChIP-chip analysis shows enrichment of *CAB1*, *CHS*, and *RbcS1A*, which was confirmed by ChIP-PCR. Input control is shown at bottom.
(B) Quantitative real-time PCR analysis confirms the ChIP-PCR results. The enrichment of the promoter regions of *CAB1*, *CHS*, *RbcS1A*, and *F3H* was confirmed by real-time PCR using the ChIP products from the wild type and *HA:HY5*. Values are normalized against wild-type values and are means of triplicate experiments with error bars representing SD. Negative control (At4g26900) data are shown at right.
(C) RNA gel blot analysis in the wild type and *hy5* after the dark-to-light transition. Seedlings were grown in the dark for 4 d, then transferred to white light (80 $\mu mol \cdot m^{-2} \cdot s^{-1}$).
(D) RNA gel blot analysis in wild-type and *hy5* seedlings grown under Wc light.
(E) Accumulation rates of chlorophyll (top) and anthocyanin (bottom) after the dark-to-light transition. Wild-type (closed squares) and *hy5* mutant (open circles) seedlings were grown in the dark for 4 d, then transferred to white light (closed circles); tissues were harvested at 0, 6, 12, and 24 h after transfer.

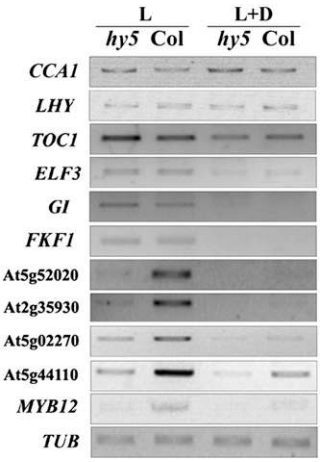

Figure 9. Effects of *hy5* and the Light-to-Dark Transition on the Expression of Genes Encoding Circadian Regulators.

Wild-type and *hy5* plants were grown under continuous white light (L) for 4 d and transferred to darkness (D) for 8 h. The expression of genes for circadian regulators (*CCA1*, *LHY*, *TOC1*, *ELF3*, *GI*, and *FKF1*) and randomly selected HY5 target genes (At5g52020, At2g35930, At5g02270, At5g44110, and *MYB12*) among the genes downregulated by *hy5* was detected by RT-PCR. *Tubulin* (*TUB*) was used as a quantitative control.

from in vitro binding analysis were included in the HY5 binding targets in this work. This fact clearly shows the limitations of in vitro analysis. As shown in our ChIP-chip analysis, ~30% of target promoters do not have a recognizable HY5 binding consensus sequence, suggesting that chromatin structure also affects the binding of transcription factors. This finding highlights the importance of ChIP-chip analysis, because a large fraction of native binding sites can only be determined empirically and not by searching consensus binding motifs defined by in vitro tests.

Genome-Wide Binding Characteristics of a Transcription Factor in *Arabidopsis*

Approximately two-thirds of HY5 binding sites were located at intergenic regions, where either one or both promoters of neighboring genes are found. Among them, 65% were located <1 kb upstream and 82% were located <2 kb upstream of the transcriptional start site, which strongly supports the conclusion that HY5 preferentially binds to promoter regions. This result was similar to that of the genome-wide binding analysis of transcription factor Rap1 in yeast (Lieb et al., 2001). Although Rap1 binding sites were found in both coding and intergenic sequences, binding of Rap1 was strongly biased toward the intergenic regions, where promoters are located. However, unbiased mapping in human chromosomes 21 and 22 showed that only a small fraction of transcription factor binding sites is located in the region proximal to the 5′ ends (<5 to 10 kb upstream from the 5′ ends), and the majority of binding sites were located in introns, near 3′ ends, and even at unannotated regions (Weinmann et al., 2002; Martone et al., 2003; Cawley et al., 2004; Euskirchen et al., 2004). This may reflect the simplicity of genome structure in *Arabidopsis* (Arabidopsis Genome Initiative, 2000). Because the average distance between two neighboring genes in *Arabidopsis* is 5 kb and the size of the introns and intergenic regions is relatively small (similar to that of yeast), the transcription factor binding at introns or 3′ ends in yeast and *Arabidopsis* may have been minimized by preferential binding at promoters. Alternatively, during the evolutionary process to reduce genome complexity in *Arabidopsis*, the transcription factor binding at the promoter regions may have been preferentially selected for the efficient regulation of transcription. A recent ChIP-chip analysis for TGA2 in *Arabidopsis* also showed that a small fraction of binding sites lay outside of the presumptive promoter regions (Thibaud-Nissen et al., 2006).

HY5 Function at a High Hierarchical Level in Photomorphogenesis

Genome-wide analysis using ChIP-chip revealed a large number of HY5 binding targets that are involved in diverse developmental processes. Considering that HY5 protein plays a pivotal role in photomorphogenesis, this may not be surprising. The genome-wide HY5 binding site analysis shows that HY5 contributes to both early- and late-responsive gene expression. ChIP-chip analysis shows that HY5 binds directly to the promoters of those genes related to photosynthesis, such as *CAB1*, *F3H*, *RbcS1A*, and *CHS*. Moreover, it was shown that HY5 is necessary for the rapid transcription of those genes during the dark-to-light transition, which eventually allows the accumulation of chlorophyll and anthocyanin for photosynthesis (Figure 8).

It was suggested that the activation of a photoreceptor sets off a transcriptional cascade by regulating a master set of transcription factors (Tepperman et al., 2001, 2004). Interestingly, >60% of early-induced genes by phyA or phyB are HY5 binding targets (Figure 7). This strongly supports the notion that HY5 is one of the high hierarchical regulators of the transcriptional cascade for photomorphogenesis. Our results also showed that many transcription factors mediating auxin signaling, ethylene signaling, and gibberellin signaling are among the HY5 binding targets, which implies that HY5 integrates light and hormone signaling in the control of gene expression.

HY5 Binding Is Not Sufficient for Transcriptional Regulation

The transcription of *CHS* and *RbcS1A* is induced by light as a result of the presence of light-inducible *cis* elements on the promoters (Giuliano et al., 1988). However, our light-to-dark transition experiment showed that HY5 binds to the promoters of *CHS* and *RbcS1A* even during dark periods. Such constitutive binding of HY5 indicates that HY5 binding alone cannot activate the transcription of *CHS* and *RbcS1A*. A more dramatic example can be seen in the binding of HY5 at the promoters of circadian oscillators. The circadian rhythm is maintained by a feedback loop involving two types of oscillators, *TOC1* and *ELF4*, for which transcription peaks at dusk, and *CCA1* and *LHY*, for which transcription peaks at dawn (Yanovsky and Kay, 2003). It was suggested that TOC1 and ELF4 activate the transcription of *CCA1* and *LHY* and that CCA1 and LHY suppress the transcription of *TOC1* and *ELF4* and that such a feedback loop sustains the circadian rhythms. However, HY5 binds to the promoters of

all four of these oscillators, which have different circadian rhythms in their own gene expression. Furthermore, HY5 binding to the promoters of these genes was similar at dawn and dusk during daily rhythms (see Supplemental Figures 2 and 3 online). This result demonstrates that HY5 binding is not sufficient for transcriptional activation but suggests that some other cofactors or modification of HY5 may be necessary for the transcriptional regulation. It is noteworthy that HY5 can be phosphorylated in darkness and that the phosphorylated HY5 is physiologically less active (Hardtke et al., 2000). Thus, phosphorylation is one of the possible mechanisms of the transcriptional regulation of HY5. The constitutive binding of transcription factor is also observed in the ChIP-chip analyses of both yeast and human systems, such that the binding of transcription factors is not changed by environmental conditions affecting transcriptional activity or is not correlated with transcriptional status (Horak and Snyder, 2002; Weinmann et al., 2002; Martone et al., 2003; Cawley et al., 2004; Euskirchen et al., 2004).

Possible Regulation Modes of HY5

Our results support the notion that HY5 is a high hierarchical regulator of the transcriptional cascades for photomorphogenesis, especially by inducing more transcription factors in the early-responsive stages. How exactly HY5 functions during photomorphogenesis is still an open question.

Recently, MYB12 (At2g47460), which is in our HY5 binding target collection and is regulated by HY5 (Figure 9), was reported as a transcriptional activator of *CHS* (Mehrtens et al., 2005), similar to HY5. Either the *hy5* or *myb12* mutant can lead to the downregulation of *CHS*, which suggests that both HY5 and MYB12 are essential for the activation of *CHS*. As illustrated in Supplemental Figure 4 online, HY5 activates a downstream transcription factor, *MYB12*, and then together with it activates the target gene *CHS*. In another case, bZIP factor GBF1 (ZBF2, At4g36730), which was recently reported as an activator of photomorphogenesis specifically under blue light (Mallappa et al., 2006), is also in our HY5 binding target list.

Besides the activators for photomorphogenesis, MYC2 (ZBF1, At1g32640), a bHLH protein that functions as a common transcriptional regulator in light and abscisic acid and jasmonic acid hormone signaling pathways, also shows high enrichment in its promoter by HY5 in our ChIP-chip analysis. MYC2 acts as a negative transcriptional regulator in blue light signaling and as a positive regulator for lateral root formation (Yadav et al., 2005). Considering that HY5 acts as a positive regulator of blue light signaling and as a negative regulator for lateral root formation (Oyama et al., 1997; Cluis et al., 2004), it is possible for them to act antagonistically to the same targets.

Interestingly, Yadav et al. (2005) found that MYC2 is able to use either the Z or G box as a binding site. In our binding motif analysis, the Z box was also enriched in the promoter region of HY5 target genes. Considering the constitutive expression of *MYC2* in dark- and light-grown *Arabidopsis* seedlings and its negative regulation of photomorphogenesis (Yadav et al., 2005), one possibility is that HY5 may partly take over the role of MYC2 in the light pathway to activate some G box–containing genes (*CHS*, *Rbcs1A*, etc.) after light irradiation by competitively occupying the G box. Hartmann et al. (2005) reported that differential combinatorial interactions of three kinds of *cis* elements (MYB recognition elements [MREs], ACGT-containing elements [ACEs], and R response elements [RREs]) are crucial for the complex expression pattern of phenylpropanoid biosynthesis genes. MRE and RRE can be recognized by MYB and bHLH factors, respectively, whereas ACE can be recognized by both bZIP and bHLH factors. It is worth noting here that ACEs could be either a G box (cACGTg) or a Z box (tACGTg). The *CHS* gene contains all three *cis* elements in the promoter region. Thus, it is possible that HY5 regulates some transcription factor expression and then, in various combinations with those target transcription factors, regulates the downstream target genes.

Although this genome-wide analysis of HY5 binding sites advances our understanding of photomorphogenesis and the function of HY5, it also reveals the complexity of how a higher plant transcription factor works at the genome scale. This complexity can be observed based on the huge number of HY5 in vivo binding sites, and expression for many of those target genes is not light-regulated. The functional role of those target genes needs to be studied further. The putative target genes of HY5 in vivo include all sorts of functional groups and many other transcription factors as well, with some also involved in regulating photomorphogenesis. Thus, ChIP-chip analysis provides a new starting point to further our understanding of this developmental process at the whole genome scale.

METHODS

Plant Materials and Growth Conditions

The wild type used was *Arabidopsis thaliana* strain Columbia, and all of the mutants and transgenic lines are in the Columbia background. The mutant *hy5-Ks50*, *hy5-221*, and *35S-HY5* transgenic lines were described previously (Oyama et al., 1997; Hardtke et al., 2000), and the mutation of *hy5-Ks50* was introduced into Columbia by genetic backcrossing. Seed sterilization and plant growth conditions were as described previously (Hardtke et al., 2000). Three-day cold-treated seeds were exposed to white light for 12 h, then transferred to Wc (180 $\mu mol \cdot m^{-2} \cdot s^{-1}$), FRc (140 $\mu mol \cdot m^{-2} \cdot s^{-1}$), Rc (80 $\mu mol \cdot m^{-2} \cdot s^{-1}$), or continuous blue (Bc) (4 $\mu mol \cdot m^{-2} \cdot s^{-1}$) light.

Generation of the *35S-HA:HY5* Transgenic Line

To generate a *35S-HA:HY5* construct, *HY5* cDNA was amplified by PCR using the *35S-HY5* construct (Hardtke et al., 2000) with two primers, 5′-TAGCCGGCATGCAGGAACAAGCGACTAGCT-3′ and 5′-TAGTCGACGAGCTCTCAAAGGCTTGCATCAGCATTA-3′, that include *Nae*I and *Sac*I sites at the 5′ and 3′ ends of *HY5*, respectively. Three copies of the HA tag were amplified by PCR with *Kpn*I and *Eco*RV restriction enzyme sites at the 5′ and 3′ ends and ligated with amplified *HY5* cDNA in frame after cutting with *Eco*RV and *Nae*I, respectively, then inserted into the *Kpn*I and *Sac*I sites of pJIM19(Kan), a binary vector based on pBIN19 with 35S promoter of cauliflower mosaic virus and kanamycin resistance markers. The DNA construct was electroporated into *Agrobacterium tumefaciens* strain GV3101 and used for *hy5-Ks50* homozygous mutant transformation by the vacuum infiltration method.

ChIP

ChIP was performed on 4-d-old seedlings grown under Wc, FRc, Rc, or Bc light. Seedling tissues (1.5 g) were cross-linked with 50 mL of 1%

formaldehyde in a vacuum for 15 min. A total of 2.5 mL of 2 M Gly was added to stop the cross-linking. After rinsing seedlings with water, tissues were ground with liquid nitrogen and resuspended with 25 mL of extraction buffer I (0.4 M sucrose, 10 mM Tris-HCl, pH 8, 10 mM $MgCl_2$, 5 mM β-mercaptoethanol, 0.1 mM phenylmethylsulfonyl fluoride [PMSF], and 1× protease inhibitor; Roche), then filtered through Miracloth (Calbiochem). The filtrate was centrifuged at 4000 rpm at 4°C for 20 min. The pellet was resuspended in 1 mL of extraction buffer II (0.25 M sucrose, 10 mM Tris-HCl, pH 8, 10 mM $MgCl_2$, 1% Triton X-100, 5 mM β-mercaptoethanol, 0.1 mM PMSF, and 1× protease inhibitor) and centrifuged at 14,000 rpm and 4°C for 10 min. The pellet was resuspended in 300 μL of extraction buffer III (1.7 M sucrose, 10 mM Tris-HCl, pH 8, 0.15% Triton X-100, 2 mM $MgCl_2$, 5 mM β-mercaptoethanol, 0.1 mM PMSF, and 1× protease inhibitor) and loaded on top of an equal amount of clean extraction buffer III, then centrifuged at 14,000 rpm for 1 h. The crude nuclear pellet was resuspended in nuclear lysis buffer (50 mM Tris-HCl, pH 8.0, 10 mM EDTA, 1% SDS, and 1× Complete protease inhibitor; Roche) and sonicated with a Branson sonifier (VWR) to achieve an average fragment size of ~0.3 to 1.0 kb. The sonicated chromatin was centrifuged, and the insoluble pellet was discarded. The soluble chromatin solution was diluted 10-fold with ChIP dilution buffer (1.1% Triton X-100, 1.2 mM EDTA, 16.7 mM Tris-HCl, pH 8.0, and 167 mM NaCl), then after preclearing with protein A–Sepharose beads (Sigma-Aldrich), 5 μL of HY5 or HA tag–specific monoclonal antibody (Santa Cruz Biotechnology) was added to 1 mL of chromatin solution and incubated overnight at 4°C. The immunocomplexes were extracted by incubating with 100 μL of 50% protein A–Sepharose beads for 1 h at 4°C. After several washes, immunocomplex was eluted twice from the beads with 250 μL of elution buffer (1% SDS and 0.1 M $NaHCO_3$), then reverse cross-linked with a final concentration of 200 mM NaCl at 65°C for 6 to 8 h. After removing all proteins by treating with proteinase K, DNA was purified by phenol-chloroform extraction and followed by ethanol precipitation. The pellet was resuspended with 50 μL of 0.1× TE (10 mM Tris-EDTA, pH 7.5) with RNase A (0.1 mg/mL) and used for probe synthesis or PCR analysis. A small aliquot of untreated sonicated chromatin was reverse cross-linked and used as the total input DNA control.

Quantitative Real-Time PCR

ChIP DNA samples of the wild type (Columbia) and *HA:HY5* were analyzed by quantitative real-time PCR. Primers were designed to amplify 130- to 300-bp DNA fragments. The details of oligonucleotides for PCR are described in Supplemental Table 2 online. Quantitative PCR was performed in 96-well format using an Applied Biosystems 7300 Fast Real-Time PCR system and SYBR Green Master Mix (Bio-Rad). Cycling conditions were as follows: 8 min at 95°C, 40 cycles of 10 s at 95°C, 30 s at 58°C, and 30 s at 72°C, followed by a 60 to 95°C dissociation protocol. The $-\Delta\Delta Ct$ values were calculated relative to reference PCR values (Livak and Schmittgen, 2001).

High-Density Oligomer Microarray Design

Using maskless array synthesizer technology (Singh-Gasson et al., 1999), we constructed a high-density oligonucleotide microarray to represent the whole *Arabidopsis* genome. A total of 193,751 60-nucleotide probes, positioned every 500 ± 25 nucleotides along one strand of the genome, and random control probes and 105 duplicated probes were selected to synthesize 194,017 features on a single array. The probes with repetition frequency > 3 (Stolc et al., 2005) were filtered out to make the number of probes fit on one microarray chip.

Probe Labeling

The DNA product obtained by ChIP was amplified and labeled as described previously with minor modifications (Iyer et al., 2001). In brief, 7 μL of ChIPed DNA was mixed with 2 μL of 5× Sequenase buffer and 1 μL of 50 μM primer 1 (5′-GTTTCCCAGTCACGATCNNNNNNNNN-3′) and incubated at 94°C for 2 min, followed by cooling to 8°C; then, 5 μL of reaction mixture (1× Sequenase buffer, 0.15 mM deoxynucleotide triphosphate [dNTP], 0.015 M DTT, 0.75 μg of BSA, and 0.3 μL of Sequenase [U.S. Biochemical]) was added. The temperature of the mixture was increased to 37°C over 8 min, then kept at 37°C for 8 min for polymerization. The DNA in the mixture was denatured at 94°C for 2 min and cooled to 8°C, and 0.24 μL of Sequenase was added. The temperature was increased to 37°C over 8 min and kept at 37°C for 8 min for polymerization again. The DNA was diluted to 50 μL with 1× TE buffer. From the diluted DNA, 15 μL was used for the first PCR and mixed with 10 μL of 10× PCR buffer, 2.5 μL of 10 mM dNTP, 2 μL of 25 mM $MgCl_2$, 2.5 μL of 50 μM primer 2 (5′- GTTTCCCAGTCACGATC-3′), and 1 μL of Taq polymerase (Qiagen) and water to make 100 μL of total solution. The first PCR was performed with following conditions: 18 to 20 cycles of 92°C for 30 s, 40°C for 30 s, 50°C for 30 s, and 72°C for 2 min. The second PCR for incorporating aminoallyl-dUTP was performed using 15 μL of the first PCR product, mixed with 5 μL of 10× PCR buffer, 0.5 μL of 50× dNTP mixture (10 μL each of 100 mM dA, dC, and dG, 2 μL of 100 mM dTTP, and 8 μL of 100 mM aminoallyl-dUTP), 1 μL of 25 mM $MgCl_2$, 1 μL of 50 μM primer 2, 0.5 μL of Taq polymerase, and water to make 50 μL of total solution with the same PCR conditions described above. After purifying the PCR product using Microcon-30 filters, 7 μL (1 to 2 μg) of purified DNA was mixed with 0.7 μL of 1 M sodium bicarbonate, pH 9.0, and 1 μL of Cy5 or Cy3 dye (Amersham; dissolved in DMSO), incubated for 90 min at room temperature in the dark, and then quenched with 1 μL of 2 M ethanolamine (Sigma-Aldrich) by incubation for 15 min. The labeled products were purified with a QiaQuick PCR purification column (Qiagen).

Microarray Hybridization

Microarray chips were prehybridized with prehybridization buffer (33.3 mM MES, 0.33 M Na^+, 6.6 mM EDTA, 0.03% Tween 20, 0.03 mg/mL salmon sperm DNA, and 0.17 mg/mL BSA) for 15 min at 45°C. Arrays were washed with water twice and hybridized with labeled DNA in hybridization buffer (50 mM MES, 0.5 M NaCl, 10 mM EDTA, 0.005% [v/v] Tween 20, 0.1 mg/mL salmon sperm DNA, and 0.5 mg/mL BSA) for 14 to 16 h at 57°C. After hybridization, the arrays were washed in nonstringent buffer (6× SSPE [1× SSPE is 0.115 M NaCl, 10 mM sodium phosphate, and 1 mM EDTA, pH 7.4] and 0.01% [v/v] Tween 20) for 3 min at room temperature, then in stringent buffer (100 mM MES, 0.1 M NaCl, and 0.01% Tween 20) for 20 min at 45°C. Arrays were rinsed three times with nonstringent buffer at room temperature and once with ice-chilled stringent buffer, then dried by centrifugation (1000 rpm, 5 min). Microarrays were scanned with a GenePix 4000B scanner (Axon), and independent TIFF images for both Cy-3 and Cy-5 channels were acquired at 5 μm resolution.

Microarray Data Analysis

The microarrays were scanned with GENEPIX Pro 3.0 software, and intensity data were extracted with NimbleScan software (NimbleGen Systems). The signal intensities were normalized by the loess normalization method before further analysis (Yang et al., 2002). A linear model was used to estimate experimental effects and to remove the variation caused by global and oligonucleotide-specific array and dye effects to create a corrected signal for each oligonucleotide. The ratio of corrected signals was then used to assess changes in fluorescence intensity between ChIP DNA and input DNA. It was assumed that the oligonucleotides representing a HY5 binding target will give a ratio of ChIP DNA and input DNA significantly >1. A moderated *t* statistic was computed to detect oligonucleotides undergoing significant changes. Then, the false-discovery

rate controlling method (Benjamini and Hochberg, 1995) was used to control for multiple testing errors. The linear model and statistical procedure were provided and implemented according to the limma package for R (Smyth et al., 2005).

All of the oligonucleotides were sorted according to their positions on Final Release 5 of the *Arabidopsis* genome annotation data from The Institute for Genomic Research (Haas et al., 2005) using National Center for Biotechnology Information megablast (Altschul et al., 1997). Then, we used two different criteria derived from the two known HY5 binding targets, *CHS* and *RbcS1A*, to identify HY5 binding targets: (1) if a gene contains at least one oligonucleotide in the promoter or coding region with fold change > 2 and $P < 0.001$; (2) if a gene contains multiple oligonucleotides (≥ 2) with fold change > 1.5 and $P < 0.01$. If two adjacent genes shared a common promoter region, the region was divided into two parts that were assigned to the corresponding gene.

Using the gene position information from The Institute for Genomic Research annotation data, we plotted all of the genes without internal structure information using a perl script, each gene corresponding to a bar in Figure 3B. Green and yellow were used for normal genes and pseudogenes, respectively.

Promoter Motif Analysis

Up to 2-kb sequences upstream of the HY5 target genes defined above were extracted, and a self-written perl script with regular expression algorithm was used to search some known TF binding sites, such as G box, C box, CG hybrid, CA hybrid (Hong et al., 2003), and Z box, in the HY5 target genes with the whole genome as a control. The percentage of genes that contain the four kinds of motifs among HY5 target genes and the whole genome was summarized (Figure 3D). MDscan (Liu et al., 2002) and Weeder (Pavesi et al., 2004) was also used to discover the novel consensus motif of HY5 binding target genes.

Target Gene Ontology Analysis

Functional categories of the HY5 target genes were classified, and the percentage of each category was compared with the whole genome data using the Munich Information Center for Protein Sequences functional categories (FunCat) website (Ruepp et al., 2004). Transcription factors were selected according to the Database of Arabidopsis Transcription Factors (Guo et al., 2005) *Arabidopsis* transcription factors list, then the hypergeometric test was used to compare the HY5 target genes and the whole genome data (Figure 4). The possibility (p) of being transcription factors is defined by the following equation:

$$p = \frac{\binom{M}{x}\binom{N-M}{n-x}}{\binom{N}{n}},$$

where M is the number of all transcription factors in the *Arabidopsis* genome, N is the gene number in *Arabidopsis*, and x is the number of HY5 target genes.

Confirmation with ChIP-PCR

The ChIP products were resuspended with 50 μL of TE, and 1 μL was used for PCR with the primers listed in Supplemental Table 2 online. PCR conditions were as follows: 94°C for 3 min, 30 cycles of 94°C for 30 s, 55°C for 30 s, and 72°C for 30 s, followed by 72°C for 10 min. Sonicated total input DNA (0.5%) was used for PCR for quantitative control.

Protein Gel Blot and RNA Expression Analysis

Total protein extraction, nuclear fractionation, and protein gel blot analysis were performed as described previously (Osterlund et al., 2000; Cho et al., 2006). For RNA expression analysis, RNA gel blot analysis and reverse transcription–coupled PCR analysis were performed according to the procedures described previously (Moon et al., 2005; Ryu et al., 2005). The cDNA probes of *CAB1*, *CHS*, and *RbcS1A* were synthesized from reverse transcription–coupled PCR. Details of the oligonucleotides used for PCR are listed in Supplemental Table 2 online.

Phenotype Analysis

To measure chlorophyll and anthocyanin accumulation, the seedlings were grown on Murashige and Skoog agar plates for 4 d under dark conditions and transferred to white light (80 $\mu mol \cdot m^{-2} \cdot s^{-1}$), then incubated for 0, 6, 12, and 24 h. The amounts of chlorophyll and anthocyanin were measured as described previously (Kim et al., 2003).

Accession Numbers

Sequence data for the ChIP-chip data and the expression profiling data of wild-type *HY5* and the *hy5* mutant can be found in the Gene Expression Omnibus database under accession numbers GSE6510 and GSE6517, respectively.

Supplemental Data

The following materials are available in the online version of this article.

Supplemental Figure 1. Independent Confirmation of Putative HY5 Targets Derived from ChIP-Chip Data.

Supplemental Figure 2. HY5 Binding to the Promoters of Circadian Regulator Genes.

Supplemental Figure 3. Daily Rhythm of HY5 Binding to the Promoters of the Genes Involved in Circadian Rhythms.

Supplemental Figure 4. Some Possible Regulation Modes of HY5.

Supplemental Table 1. List of 3894 HY5 Binding Sites.

Supplemental Table 2. Oligonucleotide Sequences for the Primer Pairs Used in ChIP-PCR Confirmation of Selected Gene Promoters.

Supplemental Table 3. Lists of Putative HY5 Targets Contained within the *Arabidopsis* Organ-Specific Light Regulation of Genome Expression Data Set (Ma et al., 2005) and the FRc and Rc Light–Regulated Gene Data Sets (Tepperman et al., 2001, 2004).

ACKNOWLEDGMENTS

This work was supported by National Institutes of Health Grant GM-47850 to X.W.D., by Grant R02-2003-000-10020-0 from the Basic Research Program of the Korea Science and Engineering Foundation, by Grant C00044 from the Korea Research Foundation, by Grant M10600000164-06J0000-16410 from the Korea Science and Engineering Foundation through the National Research Laboratory Program, by a grant from the Seoul Research and Business Development Program, and by a grant from the Korea Science and Engineering Foundation through the Plant Metabolism Research Center, Kyung Hee University, to I.L. J.L. was supported by the International Research Internship Program of the Korea Science and Engineering Foundation. K.H. was a Peking–Yale Center Monsanto Fellow and was supported by the 973 National Key Basic Research Program of China (Grant 2003CB715900) and the Natural Science Foundation of China (Grant 90408015).

Received September 25, 2006; revised December 14, 2006; accepted February 7, 2007; published March 2, 2007.

REFERENCES

Altschul, S.F., Madden, T.L., Schaffer, A.A., Zhang, J., Zhang, Z., Miller, W., and Lipman, D.J. (1997). Gapped BLAST and PSI-BLAST: A new generation of protein database search programs. Nucleic Acids Res. **25:** 3389–3402.

Anderson, S.L., Somers, D.E., Millar, A.J., Hanson, K., Chory, J., and Kay, S.A. (1997). Multiple genetically defined phototransduction pathways interact with circadian clock signals to regulate CAB2 transcription. Plant Cell **9:** 1727–1743.

Ang, L.H., Chattopadhyay, S., Wei, N., Oyama, T., Okada, K., Batschauer, A., and Deng, X.W. (1998). Molecular interaction between COP1 and HY5 defines a regulatory switch for light control of *Arabidopsis* development. Mol. Cell **1:** 213–222.

Arabidopsis Genome Initiative (2000). Analysis of the genome sequence of the flowering plant *Arabidopsis thaliana.* Nature **408:** 796–815.

Benjamini, Y., and Hochberg, Y. (1995). Controlling the false discovery rate: A practical and powerful approach to multiple testing. J. R. Stat. Soc. B **57:** 289–300.

Buck, M.J., and Lieb, J.D. (2004). ChIP-chip: Considerations for the design, analysis, and application of genome-wide chromatin immunoprecipitation experiments. Genomics **83:** 349–360.

Cawley, S., et al. (2004). Unbiased mapping of transcription factor binding sites along human chromosomes 21 and 22 points to widespread regulation of noncoding RNAs. Cell **116:** 499–509.

Chattopadhyay, S., Ang, L.H., Puente, P., Deng, X.W., and Wei, N. (1998). Arabidopsis bZIP protein HY5 directly interacts with light-responsive promoters in mediating light control of gene expression. Plant Cell **10:** 673–683.

Chen, M., Chory, J., and Fankhauser, C. (2004). Light signal transduction in higher plants. Annu. Rev. Genet. **38:** 87–117.

Cho, Y.-H., Yoo, S.D., and Sheen, J. (2006). Regulatory functions of nuclear hexokinase1 complex in glucose signaling. Cell **127:** 579–589.

Cluis, C.P., Mouchel, C.F., and Hardtke, C.S. (2004). The Arabidopsis transcription factor HY5 integrates light and hormone signaling pathways. Plant J. **38:** 332–347.

Euskirchen, G., Royce, T.E., Bertone, P., Martone, R., Rinn, J.L., Nelson, F.K., Sayward, F., Luscombe, N.M., Miller, P., Gerstein, M., Weissman, S., and Snyder, M. (2004). CREB binds to multiple loci on human chromosome 22. Mol. Cell. Biol. **24:** 3804–3814.

Euskirchen, G., and Snyder, M. (2004). A plethora of sites. Nat. Genet. **36:** 325–326.

Gao, Y., Li, J., Strickland, E., Hua, S., Zhao, H., Chen, Z., Qu, L., and Deng, X.W. (2004). An Arabidopsis promoter microarray and its initial usage in the identification of HY5 binding targets *in vitro.* Plant Mol. Biol. **54:** 683–699.

Giuliano, G., Pechersky, E., Malik, V.S., Timko, M.P., Scolnik, P.A., and Cashmore, A.R. (1988). An evolutionarily conserved protein binding sequence upstream of a plant light-regulated gene. Proc. Natl. Acad. Sci. USA **85:** 7089–7093.

Guo, A., He, K., Liu, D., Bai, S., Gu, X., Wei, L., and Luo, J. (2005). DATF: A database of *Arabidopsis* transcription factors. Bioinformatics **21:** 2568–2569.

Haas, B.J., Wortman, J.R., Ronning, C.M., Hannick, L.I., Smith, R.K., Maiti, R., Chan, A.P., Yu, C., Farzad, M., Wu, D., White, O., and Town, C.D. (2005). Complete reannotation of the Arabidopsis genome: Methods, tools, protocols and the final release. BMC Biol. **3:** 7.

Hardtke, C.S., Gohda, K., Osterlund, M.T., Oyama, T., Okada, K., and Deng, X.W. (2000). HY5 stability and activity in Arabidopsis is regulated by phosphorylation in its COP1 binding domain. EMBO J. **19:** 4997–5006.

Hartmann, U., Sagasser, M., Mehrtens, F., Stracke, R., and Weisshaar, B. (2005). Differential combinatorial interactions of ACE-, MRE- and RRE-binding transcription factors control light-responsive and tissue-specific activation of phenylpropanoid biosynthesis genes. Plant Mol. Biol. **57:** 155–171.

Hicks, K.A., Albertson, T.M., and Wagner, D.R. (2001). *EARLY FLOWERING3* encodes a novel protein that regulates circadian clock function and flowering in Arabidopsis. Plant Cell **13:** 1281–1292.

Holm, M., Ma, L.G., Qu, L.J., and Deng, X.W. (2002). Two interacting bZIP proteins are direct targets of COP1-mediated control of light-dependent gene expression in *Arabidopsis.* Genes Dev. **16:** 1247–1259.

Hong, J.C., Kim, S.H., and Song, Y.H. (2003). Protein-DNA and protein-protein interactions of STF1, a bZIP protein homologous to HY5. Proc. Kumho Life Environ. Sci. Lab. Workshop **8:** 39–49.

Horak, C.E., and Snyder, M. (2002). ChIP-chip: A genomic approach for identifying transcription factor binding sites. Methods Enzymol. **350:** 469–483.

Iyer, V.R., Horak, C.E., Scafe, C.S., Botstein, D., Snyder, M., and Brown, P.O. (2001). Genomic binding sites of the yeast cell-cycle transcription factors SBF and MBF. Nature **409:** 533–538.

Jang, I.-C., Yang, J.-Y., Seo, H.S., and Chua, N.-H. (2005). HFR1 is targeted by COP1 E3 ligase for post-translational proteolysis during phytochrome A signaling. Genes Dev. **19:** 593–602.

Kendrick, R.E., and Kronenberg, G.H.M. (1994). Photomorphogenesis in Plants. (Dordrecht, The Netherlands: Kluwer Academic Publishers).

Kim, J., Yi, H., Choi, G., Shin, B., Song, P.-S., and Choi, G. (2003). Functional characterization of phytochrome interacting factor 3 in phytochrome-mediated light signal transduction. Plant Cell **15:** 2399–2407.

Koornneef, M., Rolff, E., and Spruit, C.J.P. (1980). Genetic control of light-inhibited hypocotyl elongation in *Arabidopsis thaliana* (L.) Heynh. Z. Pflanzenphysiol. **100:** 147–160.

Lieb, J.D., Liu, X., Botstein, D., and Brown, P.O. (2001). Promoter-specific binding of Rap1 revealed by genome-wide maps of protein–DNA association. Nat. Genet. **28:** 327–334.

Liu, X.S., Brutlag, D.L., and Liu, J.S. (2002). An algorithm for finding protein–DNA binding sites with applications to chromatin-immunoprecipitation microarray experiments. Nat. Biotechnol. **20:** 835–839.

Livak, K.J., and Schmittgen, T.D. (2001). Analysis of relative gene expression data using real-time quantitative PCR and the 2(-Delta Delta C(T)) method. Methods **25:** 402–408.

Ma, L., Li, J., Qu, L., Chen, Z., Zhao, H., and Deng, X.W. (2001). Light control of Arabidopsis development entails coordinated regulation of genome expression and cellular pathways. Plant Cell **13:** 2589–2607.

Ma, L., Sun, N., Liu, X., Jiao, Y., Zhao, H., and Deng, X.W. (2005). Organ-specific expression of Arabidopsis genome during development. Plant Physiol. **138:** 80–91.

Mallappa, C., Yadav, V., Negi, P., and Chattopadhyay, S. (2006). A basic leucine zipper transcription factor, G-box-binding factor 1, regulates blue light-mediated photomorphogenic growth in Arabidopsis. J. Biol. Chem. **281:** 22190–22199.

Martone, R., Euskirchen, G., Bertone, P., Hartman, S., Royce, T.E., Luscombe, N.M., Rinn, J.L., Nelson, F.K., Miller, P., Gerstein, M., Weissman, S., and Snyder, M. (2003). Distribution of NF-κB-binding sites across human chromosome 22. Proc. Natl. Acad. Sci. USA **100:** 12247–12252.

Mehrtens, F., Kranz, H., Bednarek, P., and Weisshaar, B. (2005). The Arabidopsis transcription factor MYB12 is a flavonol-specific regulator of phenylpropanoid biosynthesis. Plant Physiol. **138:** 1083–1096.

Moon, J., Kim, M., Lee, H., and Lee, I. (2005). Analysis of flowering pathway integrators in Arabidopsis. Plant Cell Physiol. **46:** 292–299.

Obayashi, T., Okegawa, T., Sasaki-Sekimoto, Y., Shimada, H., Masuda, T., Asamizu, E., Nakamura, Y., Shibata, D., Tabata, S., Takamiya, K.-i., and Ohta, H. (2004). Distinctive features of plant

organs characterized by global analysis of gene expression in Arabidopsis. DNA Res. **11:** 11–25.

Osterlund, M.T., Hardtke, C.S., Wei, N., and Deng, X.W. (2000). Targeted destabilization of HY5 during light-regulated development of Arabidopsis. Nature **405:** 462–466.

Oyama, T., Shimura, Y., and Okada, K. (1997). The *Arabidopsis HY5* gene encodes a bZIP protein that regulates stimulus-induced development of root and hypocotyls. Genes Dev. **11:** 2983–2994.

Pavesi, G., Mereghetti, P., Mauri, G., and Pesole, G. (2004). Weeder Web: Discovery of transcription factor binding sites in a set of sequences from co-regulated genes. Nucleic Acids Res. **32:** W199–W203.

Quail, P.H. (2002). Phytochrome photosensory signalling networks. Nat. Rev. Mol. Cell Biol. **3:** 85–93.

Ruepp, A., Zollner, A., Maier, D., Albermann, K., Hani, J., Mokrejs, M., Tetko, I., Guldener, U., Mannhaupt, G., Munsterkotter, M., and Mewes, H.W. (2004). The FunCat, a functional annotation scheme for systematic classification of proteins from whole genomes. Nucleic Acids Res. **32:** 5539–5545.

Ryu, J.S., et al. (2005). Phytochrome-specific type 5 phosphatase controls light signal flux by enhancing phytochrome stability and affinity for a signal transducer. Cell **120:** 395–406.

Saijo, Y., Sullivan, J.A., Wang, H., Yang, J., Shen, Y., Rubio, V., Ma, L., Hoecker, U., and Deng, X.W. (2003). The COP1-SPA1 interaction defines a critical step in phytochrome A-mediated regulation of HY5 activity. Genes Dev. **17:** 2642–2647.

Seo, H.S., Yang, J.-Y., Ishikawa, M., Bolle, C., Ballesteros, M.L., and Chua, N.-H. (2003). LAF1 ubiquitination by COP1 controls photomorphogenesis and is stimulated by SPA1. Nature **423:** 995–999.

Singh-Gasson, S., Green, R.D., Yue, Y., Nelson, C., Blattner, F., Sussman, M.R., and Cerrina, F. (1999). Maskless fabrication of light-directed oligonucleotide microarrays using a digital micromirror array. Nat. Biotechnol. **17:** 974–978.

Smith, H. (2000). Phytochromes and light signal perception by plants—An emerging synthesis. Nature **407:** 585–591.

Smyth, G.K., Michaud, J., and Scott, H.S. (2005). Use of within-array replicate spots for assessing differential expression in microarray experiments. Bioinformatics **21:** 2067–2075.

Stolc, V., et al. (2005). Identification of transcribed sequences in *Arabidopsis thaliana* by using high-resolution genome tiling arrays. Proc. Natl. Acad. Sci. USA **102:** 4453–4458.

Sullivan, J.A., Shirasu, K., and Deng, X.W. (2003). The diverse roles of ubiquitin and the 26S proteasome in the life of plants. Nat. Rev. Genet. **4:** 948–958.

Tepperman, J.M., Hudson, M.E., Khanna, R., Zhu, T., Chang, S.H., Wang, X., and Quail, P.H. (2004). Multiple photoreceptors mediate the light-induced reduction of GUS-COP1 from Arabidopsis hypocotyl nuclei. Plant J. **38:** 725–739.

Tepperman, J.M., Zhu, T., Chang, H.-S., Wang, X., and Quail, P.H. (2001). Multiple transcription-factor genes are early targets of phytochrome A signaling. Proc. Natl. Acad. Sci. USA **98:** 9437–9442.

Thibaud-Nissen, F., Wu, H., Richmond, T., Redman, J.C., Johnson, C., Green, R., Arias, J., and Town, C.D. (2006). Development of Arabidopsis whole-genome microarrays and their application to the discovery of binding sites for the TGA2 transcription factor in salicylic acid-treated plants. Plant J. **47:** 152–162.

Ulm, R., Baumann, A., Oravecz, A., Máté, Z., Ádám, É., Oakeley, E.J., Schäfer, E., and Nagy, F. (2004). Genome-wide analysis of gene expression reveals function of the bZIP transcription factor HY5 in the UV-B response of *Arabidopsis.* Proc. Natl. Acad. Sci. USA **101:** 1397–1402.

Wei, N., and Deng, X.W. (2003). The COP9 signalosome. Annu. Rev. Cell Dev. Biol. **19:** 261–286.

Weinmann, A.S., Yan, P.S., Oberley, M.J., Huang, T.H.-M., and Farnham, P.J. (2002). Isolating human transcription factor targets by coupling chromatin immunoprecipitation and CpG island microarray analysis. Genes Dev. **16:** 235–244.

Yadav, V., Mallappa, C., Gangappa, S.N., Bhatia, S., and Chattopadhyay, S. (2005). A basic helix-loop-helix transcription factor in Arabidopsis, MYC2, acts as a repressor of blue light-mediated photomorphogenic growth. Plant Cell **17:** 1953–1966.

Yamada, K., et al. (2003). Empirical analysis of transcriptional activity in the Arabidopsis genome. Science **302:** 842–846.

Yang, J., Lin, R., Sullivan, J., Hoecker, U., Liu, B., Xu, L., Deng, X.W., and Wang, H. (2005). Light regulates COP1-mediated degradation of HFR1, a transcription factor essential for light signaling in Arabidopsis. Plant Cell **17:** 804–821.

Yang, Y.H., Dudoit, S., Luu, P., Lin, D.M., Peng, V., Ngai, J., and Speed, T.P. (2002). Normalization for cDNA microarray data: A robust composite method addressing single and multiple slide systematic variation. Nucleic Acids Res. **30:** e15.

Yanovsky, M.J., and Kay, S.A. (2003). Living by the calendar: How plants know when to flower. Nat. Rev. Mol. Cell Biol. **4:** 265–275.